

# UC Irvine

## UC Irvine Previously Published Works

### Title

Sheets of human retinal progenitor transplants improve vision in rats with severe retinal degeneration

### Permalink

<https://escholarship.org/uc/item/7gg700qj>

### Authors

Lin, Bin  
McLelland, Bryce T  
Mathur, Anuradha  
[et al.](#)

### Publication Date

2018-09-01

### DOI

10.1016/j.exer.2018.05.017

Peer reviewed



## Sheets of human retinal progenitor transplants improve vision in rats with severe retinal degeneration

Bin Lin<sup>a</sup>, Bryce T. McLelland<sup>a</sup>, Anuradha Mathur<sup>a,1</sup>, Robert B. Aramant<sup>a</sup>, Magdalene J. Seiler<sup>a,b,\*</sup>

<sup>a</sup> Stem Cell Research Center, University of California, Irvine, United States

<sup>b</sup> Department of Physical Medicine & Rehabilitation, University of California, Irvine, United States

### ARTICLE INFO

#### Keywords:

Retinal restoration  
Retinal development  
Stem cells  
Immunodeficient rat  
Electrophysiology  
Retinal transplantation  
Optical coherence tomography  
Superior colliculus recording

### ABSTRACT

Loss of photoreceptors and other retinal cells is a common endpoint in retinal degenerate (RD) diseases that cause blindness. Retinal transplantation is a potential therapy to replace damaged retinal cells and improve vision. In this study, we examined the development of human fetal retinal sheets with or without their retinal pigment epithelium (RPE) transplanted to immunodeficient retinal degenerate *rho S334ter-3* rats. Sheets were dissected from fetal human eyes (11–15.7 weeks gestation) and then transplanted to the subretinal space of 24–31 d old RD nude rats. Every month post surgery, eyes were imaged by high-resolution spectral-domain optical coherence tomography (SD-OCT). SD-OCT showed that transplants were placed into the subretinal space and developed laminated areas or rosettes, with clear development of plexiform layers first seen in OCT at 3 months post surgery. Several months later, as could be expected by the much slower development of human cells compared to rat cells, transplant photoreceptors developed inner and later outer segments. Retinal sections were analyzed by immunohistochemistry for human and retinal markers and confirmed the formation of several retinal subtypes within the retinal layers. Transplant cells extended processes and a lot of the cells could also be seen migrating into the host retina. At 5.8–8.6 months post surgery, selected rats were exposed to light flashes and recorded for visual responses in superior colliculus, (visual center in midbrain). Four of seven rats with transplants showed responses to flashes of light in a limited area of superior colliculus. No response with the same dim light intensity was found in age-matched RD controls (non-surgery or sham surgery). In summary, our data showed that human fetal retinal sheets transplanted to the severely disturbed subretinal space of RD nude rats develop mature photoreceptors and other retinal cells, integrate with the host and induce vision improvement.

### 1. Introduction

Age-related macular degeneration (de Jong, 2006; Hanus et al., 2016), Stargardt's disease (Walia and Fishman, 2009), and retinitis pigmentosa (Hartong et al., 2006) are common RD diseases, which often result in irreversible blindness. Many treatments currently in use and in development, such as gene therapy (Bennett et al., 1996; Liu et al., 2011), and trophic factors (LaVail, 2005) show effect only in early disease stages when the host photoreceptors are damaged but still alive and can be rescued. Rescue treatments are unsuccessful when photoreceptors are irreversibly degenerated. Since retinal ganglion cells can survive after severe photoreceptor loss (Medeiros and Curcio, 2001), the most effective treatment presently would likely be to replace the photoreceptors and other retinal cells.

Extensive studies have shown that up to now, fetal donor tissue has been a very effective choice for transplantation in the central nervous system (Brundin et al., 1988; Lindvall and Bjorklund, 2011). Further studies indicated that this also applies to retinal transplantation for replacing cells of a degenerating retina (Seiler and Aramant, 1998; Ghosh et al., 1999). Fetal retina can be transplanted as dissociated cells (Huang et al., 2014), aggregates (Juliussen et al., 1993; Ivert et al., 1998; Gouras and Tanabe, 2003) and sheets (Silverman et al., 1992; Seiler and Aramant, 1998; Radtke et al., 2008; Li et al., 2009).

Later studies to transplant dissociated photoreceptor precursor cells did not report any convincing result of vision improvement (MacLaren et al., 2006; West et al., 2008, 2010; Pearson et al., 2010). Suspecting this may be due to the low numbers of photoreceptor precursors that integrated into the retina (0.2% of the injected cells; less than

\* Corresponding author. Dept. Physical Medicine & Rehabilitation, Sue & Bill Gross Stem Cell Research Center, University of California, Irvine, 845 Health Sciences Rd. 2035 Gross Hall, Irvine, CA 92697-1705, United States.

E-mail address: [mseiler@uci.edu](mailto:mseiler@uci.edu) (M.J. Seiler).

<sup>1</sup> present address: Office of Research – Research Administration; University of California, Irvine; 141 Innovation Drive, Suite 250, Irvine CA 92697-7600.

1000 cells), Pearson et al. optimized the procedure to increase the number of integrated cells to an average of 4.25% (17,000) of 400,000 injected cells. They reported that transplanted NRL-GFP mouse rod precursors formed synaptic connections with the host retina. At 4–6 weeks post transplantation (relatively short time), visual function was measured by whole-cell recording, electroretinograms, optical imaging, optomotor response and watermaze with improvements in some transplanted mice (Pearson et al., 2012).

Transplantation of dissociated cells has an advantage as the surgery is simpler than transplantation of aggregates and sheets. However, dissociated cells cannot form a laminated organization and have a limited survival long term (Juliusson et al., 1993; Mansergh et al., 2010). Transplants of cell aggregates can form rosettes but not parallel laminated layers (Juliusson et al., 1993; Ivert et al., 1998; Gouras and Tanabe, 2003).

Previous work had shown that a degenerated retinal area replaced by a fetal sheet with or without its RPE, formed laminated transplants in rodents (Seiler and Aramant, 1998; Aramant et al., 1999; Aramant and Seiler, 2002b). In several rat RD models, rat fetal-derived retinal sheet transplants restored visual responses in an area of the superior colliculus corresponding to the transplant location in the retina (Woch et al., 2001; Sagdullaev et al., 2003; Thomas et al., 2004; Seiler et al., 2010, 2017; Yang et al., 2010).

Pre-clinically, it was important to know if sheets of human fetal retina together with its RPE could be transplanted to the subretinal space. A study that used nude immunodeficient rats with normal vision showed that retinal sheet transplants with RPE could develop laminated structures after long survival times (Aramant and Seiler, 2002b), which led to the first clinical co-transplant trials (Radtke et al., 2002). In the following phase II clinical trial it was demonstrated that sheet transplants of human fetal retina with its RPE improved visual acuity in 7 of 10 patients after one year (Radtke et al., 2008). However, visual function improvement following retinal sheet transplantation had not been tested in a model of retinal degeneration. As the ultimate goal is to transplant in human patients suffering from retinal degeneration, the capability of human retinal sheet transplants to integrate into the remaining host architecture and the extent to which visual function is restored, needs to be tested in an animal model. Human tissue develops and matures at a slower rate compared to rat tissue, so the required time for experimental analysis needs to be extended. The current study aims to address these questions.

Immunosuppression is commonly applied when transplanting a xenograft such as human tissue to rats. However, immunosuppression gives unreliable results (Anderson et al., 2011), is labor-intensive and may cause pain and damage to the animals. For example, the immunosuppressant cyclosporine A can have nephrotoxic effects (Thliveris et al., 1991; Cibulskyte et al., 2005), and reduces visual responses in RCS rats (Cooper et al., 2016). Therefore, we developed a double mutant rat with a *Foxn1*<sup>-/-</sup> and *rho S334ter*<sup>-/-</sup> line-3 rhodopsin mutation (Seiler et al., 2014) which is both immunodeficient and retinal degenerate. This rat model eliminates the need for immunosuppression when transplanting xenografts and also eliminates a slow chronic immune rejection of allografts (Seiler et al., 2017).

The present study evaluated the visual function of this RD nude rat model after transplantation of human fetal retinal sheets, using extracellular recordings in the superior colliculus (SC). Transplant development and interaction between donor and host were studied using OCT and immunohistochemistry. Our data showed that transplantation of human fetal retinal sheets could improve visual function in this rat model of advanced stage of retinal degeneration.

## 2. Material and methods

### 2.1. Animals

For all experimental procedures, animals were treated in accordance

with NIH guidelines for the care and use of laboratory animals, the ARVO Statement for the Use of Animals in Ophthalmic and Vision Research, under a protocol approved by the Institutional Animal Care and Use Committee of UC Irvine. Animals were group housed in cage racks with individually filtered air. All rats were maintained on a 12 h light/dark cycle (lights on 6:30am–6:30pm) at an ambient temperature of  $21.5 \pm 0.8$  °C and a relative humidity of 50%. NIH nude rats (NTac:NIH-Foxn1rnu) were bred in-house from founder breeders purchased from Taconic (Taconic Bioscience, Inc., Hudson, NY). SD-Foxn1 Tg(S334ter)3Lav (RD nude rat) transplant recipients were generated by crossing SD-Tg(S334ter)3Lav rat and NTac:NIH-Whn rats (Seiler et al., 2014).

### 2.2. Donor tissue isolation and transplantation procedures

Human fetal eyes (11–15.7 weeks post-conception) were obtained from hSCRO approved sources after overnight shipping in hibernate E medium with B27 supplements (Life Technologies, now Thermo Fisher Scientific, Waltham, MA, USA). Donor human fetal retina was isolated in hibernate E medium and treated as previously described (Aramant and Seiler, 2002b). Briefly, donor eyes were incubated in 10% dispase for 30–40 min at 37 °C to enable the RPE and retina to be dissected free from surrounding tissues. The donor tissue was taken from different areas of the fetal retina excluding the macula since the RPE is easily detached in this area. Prior to transplantation, a small piece of donor tissue (on average 0.7 mm × 1.2 mm) was prepared and inserted into a custom-made transplantation instrument (Aramant and Seiler, 2002b). Some transplanted pieces included the attached RPE while others were retina alone. Information on the donor tissue and the transplanted rats is summarized in Table 1.

Retinal sheet transplantation was performed as previously described (Aramant and Seiler, 2002a; Yang et al., 2010). Recipient rats (P26-31, either sex) were anesthetized with Ketamine (40–55 mg/kg)/Xylazine (6.0–7.5 mg/kg). A ~1 mm incision was made posterior to the pars plana and followed by local mechanical retinal detachment. To prevent eyelid swelling, rats received a subcutaneous injection of Ketoprofen (4 mg/kg) (Zoetis Inc., Kalamazoo, MI) prior to anesthesia. The eyes were also frequently treated with dexamethasone eye drops (Bausch & Lomb Inc., Tampa) tetracaine (Bausch & Lomb Inc., Tampa FL) and Atropine eye drops (Akorn Pharmaceuticals, Lake Forest, IL). Donor retinal transplant tissue was delivered to the subretinal space of the left eye using a custom implantation instrument. The incision was closed with 10-0 sutures. Sham surgery consisted in injection of media only. For recovery, rats were given a subcutaneous injection of Ringer saline solution and were then placed in a Thermocare incubator to recover. The surgery eye was treated with Betadine and triple antibiotic ointment (neomycin/bacitracin/polymyxin). For pain management, the animals also received analgesic Buprenex (0.03 mg/kg) (Reckitt Benckiser Pharmaceuticals Inc., Richmond VA).

### 2.3. SD-OCT imaging

As described previously (Seiler et al., 2017), rats were anesthetized with ketamine/xylazine, the eyes were dilated with atropine, and SD-OCT images of the retina were obtained using a BiopTigen Envisu R2200 Spectral Domain Ophthalmic Imaging System (BiopTigen, Research Triangle Park, NC). Transplanted rats were imaged every 1–2 months from 2 weeks after surgery and with the last scan as close to the terminal experiment (SC recording) time as possible.

### 2.4. Histology and immunofluorescence

Most rats were perfusion-fixed with cold 4% paraformaldehyde in 0.1 M Na-phosphate buffer. The eye cups were processed and embedded in Tissue-Tek® O.C.T. compound and frozen using isopentane on dry ice. Serial 10 μm cryostat sections were cut and stored at –20 °C. Every fifth

**Table 1**  
Overview of experimental rats.

Rat ID	Donor age	Transplant with RPE (Y: yes. N: no)	Days post-surgery (dps) when euthanized	Age(d) when euthanized	Transplant organization: (L: laminated R: rosettes)	Response to light by SC recording (Y: yes. N: no. N/A: not recorded)
1	15 wk 5 day	N	55	81	R	N/A
2	11 wk 5 days	Y	68	95	R	N/A
3	15 wk 5 day	N	70	96	R	N/A
4	11 wk 3 day	N	99	130	L	N/A
5	11 wk 1 day	Y	175	201	R	Y
6	11 wk 1 day	N	189	215	R	Y
7	11 wk 3 day	Y	201	232	L	N
8	11 wk 5 days	Y	202	228	L *	N/A
9	11 wk 3 day	Y	207	238	L	Y
10	11 wk 5 days	Y	207	234	L	N/A
11	11 wk 3 day	Y	209	240	R	N
12	12 wk	Y	242	272	L	N
13	11 wk 5 day	N	257	284	R	Y

\*Transplant almost completely laminated; rat died before it could be recorded.

**Table 2**  
List of primary antibodies.

Antibodies	species	specific for	dilution	supplier
Bassoon	Mouse	Ribbon synapses	1:600	Stressgen (San Diego, CA)
Calretinin	Goat	Ganglion and amacrine cells	1:1000	Chemicon (Temecula, CA)
Chx10	sheep	Retinal progenitor cells	1:200	Thermo Fisher (Huntington Beach, CA)
Cone Transducin	Rabbit	Cone outer segments	1:200	Cytosignal (Irvine, CA)
CRALBP	Rabbit	Cellular retinaldehyde binding protein; RPE and Müller cells	1:1000	Dr. Saari, Univ. of WA (Saari et al., 1984)
GFAP	Mouse	Reactive Müller cells	1:100	Cell Signaling (Danvers, MA)
Iba-1	Rabbit	Microglia	1:100	Biocare Medical (Pacheco, CA)
Ku-80	Rabbit	Human nuclei	1:400	Abcam (Eugene, OR)
MAP2	Mouse	Microtubule-associated protein 2	1:100	Millipore/Chemicon (Temecula, CA)
MAP2	Rabbit	Microtubule-associated protein 2	1:500	Chemicon
NeuN	Mouse	Neuronal nuclei	1:400	Chemicon
PKC $\alpha$	Rabbit	Rod bipolar cells	1:200	Oxford Biomedical (Riviera, FL)
PKC $\alpha$	Mouse	Rod bipolar cells	1:50	Amersham (Little Chalfont, U.K.)
OTX2	Rabbit	Orthodenticle Homeobox 2	1:1000	Chemicon
Recoverin	Rabbit	Photoreceptors, cone bipolar cells	1:500	Dr. Dizhoor, Univ. PA (Dizhoor et al., 1991); Millipore/Chemicon
Red Green Opsin	Rabbit	Red and Green cones	1:2000	Chemicon
Ret. RAX	Rabbit	Retina And Anterior Neural Fold Homeobox Protein	1:200	Santa Cruz Biotechnology, Dallas, Texas
Rhodopsin (rho1D4)	Mouse	Rods	1:100	Dr. Molday, Univ. of British Columbia (Molday and MacKenzie, 1983)
Rhodopsin	Rabbit	Rods	1:2000	Dr. Plantner, Cleveland, OH (Plantner et al., 1982)
Secretagogin	Rabbit	Cone bipolar cells	1:200	Cell Signaling
$\alpha$ -Synuclein	Rabbit	Rodent amacrine cells and IPL; OLM (general)	1:100	Cell Signaling
Synaptophysin	mouse	Membrane protein of synaptic vesicles	1:500	Sigma
Synaptophysin	Goat	Membrane protein of synaptic vesicles	1:100	Novus Biologicals (Littleton, CO)
SC-121	Mouse	Cytoplasm of human cells	1:2K	Stem Cell Inc. (Newark, CA)
Vimentin	mouse	Intermediate filament present in most cells	1:500	ICN

Secondary Antibodies				
Conjugate	species	specific for	dilution	supplier
Alexa Fluor 488	Donkey	Rabbit IgG (H + L)	1:400	Jacson Immuno Research (West Grove, PA)
Rhodamine X	Donkey	Rabbit IgG (H + L)	1:400	Jacson Immuno Research
Rhodamine X	Donkey	Mouse IgG (H + L)	1:400	Jacson Immuno Research
Alexa Fluor 647	Donkey	Goat IgG (H + L)	1:400	Jacson Immuno Research

slide was stained using hematoxylin and eosin (H&E). For antigen retrieval during immunofluorescence experiments, cryostat sections were incubated for 30 min at 70 °C in HistoVT One (Nacalai Inc., San Diego, CA) Sections were blocked for at least 30 min in 10% donkey serum. Primaries were left on sections overnight at 4 °C and on the next day, sections were incubated for at least 30 min at room temperature in secondary antibodies (Jackson Immunoresearch). A list of primary and secondary antibodies is presented in Table 2. Sections were coverslipped using Vectashield mounting media (Vector Labs) with 5  $\mu$ g/mL DAPI. Fluorescent images were captured either on an Olympus BXH10 microscope, a Nikon FXA microscope or a Zeiss LSM700 confocal microscope. After taking confocal stacks of 5–8 micron thickness at 20x,

40x and 63x (selected images), Zen 2012 software was used to extract 3D confocal images in separate color channels that were later combined in Adobe Photoshop CS6 software. Volocity (x64) software (Perkin-Elmer, [www.cellularimaging.com](http://www.cellularimaging.com)) was used to obtain higher magnification 3D opacity rendered images.

### 2.5. Superior colliculus (SC) electrophysiology

Visual responses from the SC were recorded as previously described (Seiler et al., 2017). In brief, responses from selected transplanted RD nude rats were recorded between 6.6 and 9.5 months of age (5.8–8.6 months post surgery) and compared with responses from age-matched

non-transplanted RD nude and sham rats. Multi-unit electrophysiological recording was performed from 50–60 locations on the SC surface approximately 200–400  $\mu\text{m}$  apart using a tungsten microelectrode (0.5 M $\Omega$  impedance; MicroProbe, Inc, Carlsbad, CA). At each location, light stimuli (20 ms duration) were delivered approximately 10-times at 10-second intervals at an intensity of 0.58 to  $-6.13 \log \text{cd}/\text{m}^2$ . To detect the response threshold, when responses were found, the intensity of the light stimuli was reduced until there was no response. Electrophysiological responses to the strongest light stimuli (stimulus level  $0.58 \log \text{cd}/\text{m}^2$ , corresponding to 3.8 lux) were quantified and formed into a map over the area of the SC using a custom MATLAB program (Mathworks, Natick, MA). All spikes occurring 30 ms to 210 ms after the onset of the photic stimulus were counted.

## 2.6. Statistical analysis

For all statistical analyses, the significance level was calculated in Graphpad Prism software (Graphpad Software LLC, La Jolla, CA) using t-tests (paired and unpaired), Level of significance was set at 0.05.

## 2.7. Data availability statement

The datasets generated and/or analyzed during the current study are available from the corresponding author on reasonable request.

## 3. Results

### 3.1. Development and characterization of human fetal retinas

Donor tissue was isolated from five human fetuses at 11–15.7 weeks (wks) gestational age. As shown in Fig. 1, cells in the tissues were retinal progenitors, which were still developing. In a tissue at 12 weeks gestational age, strong Chx10 (Visual System Homeobox 2 protein, VSX2) staining showed retinal progenitors in the whole neuroblastic layer (NBL; Fig. 1 a). Developing ganglion cells were visible by strong MAP2 (Microtubule-associated protein 2) staining (cytoplasm of developing ganglion cells, Fig. 1 b) and NeuN (Neuronal Nuclei) staining (Fig. 1 c) in the ganglion cell layer. A layer of differentiating cone photoreceptors (based on their location close to the outer limiting membrane and the larger cell size), was strongly stained by retinal RAX (retinal Homeobox protein) (Fig. 1 b) and OTX2 (Orthodenticle Homeobox 2) antibodies (Fig. 1 c) in the outer neuroblastic layer (NBL). At this stage (12 weeks) there is no rhodopsin staining (data not shown) (Seiler and Aramant, 1994; O'Brien et al., 2003; Hoshino et al., 2017). RPE were also immunoreactive for OTX2 (Fig. 1 c). At 11 wks, only 1 layer of developing photoreceptors was stained by recoverin in the outer NBL (Fig. 1 d) but at 15.7 weeks, several layers of recoverin-positive photoreceptors were visible. Co-expression of OTX2 and Chx10 were seen in the inner NBL of a retina at 15.7 wks. Other retinal cells, such as horizontal cells (Calbindin, Fig. 1 g), RPE and Müller cells (CRALBP, cellular retinaldehyde binding protein, in Fig. 1 h and Vi-mentin in Fig. 1 i) were labeled in the human fetal retinal tissue.

### 3.2. OCT results

Thirteen of 22 rats were successfully transplanted. The transplants could be detected by OCT. As shown by OCT in Fig. 2, transplants of human fetal retinal sheets were immature at 1 month post-surgery (Fig. 2 a1 and a2) with only IPL and outer neuroblastic layers recognizable. Around 3 months post-surgery, transplants developed into visible laminated retinal layers (Fig. 2 b1 and b2). Transplants maintained the same structure until the end of experiment and with outer segments detectable in some cases (Fig. 2 c1 and c2). Six of the transplants developed laminated layers ( $n = 6$ , Fig. 2 a1-c1), and seven rosettes only ( $n = 7$ , Fig. 2 d1, d2, f1 and f2). Sometimes a mixture of both lamination and rosettes was seen (Fig. 2 e1 and e2).

Supplementary Fig. 1 shows OCT scans of rat #1 at 33, 83, and 200 dps.

Supplementary video related to this article can be found at <http://dx.doi.org/10.1016/j.exer.2018.05.017>.

### 3.3. Histology

Hematoxylin-Eosin (H-E) staining confirmed the OCT results (Fig. 3). Transplants formed laminated layers (Fig. 3 d-f and j-l), rosettes (Fig. 3 a-c) and both (Fig. 3 g-i).

#### 3.3.1. Photoreceptors

After transplantation into the subretinal space, the fetal retinal sheets developed and matured into laminated structures recognizable as IPL, INL, OPL and ONL layers. As shown in Fig. 4, matured photoreceptors with outer segments could be found in the transplants at 6 months post-surgery. Recoverin staining showed clear laminated photoreceptor layers in some transplants ( $n = 6/13$ , Fig. 4 a and b). Although most transplants formed rosette structures (spherical arrangement of retinal layers, with photoreceptors in the center,  $n = 7/13$ ), lamination within rosettes was still apparent (Fig. 4 c and d). Rhodopsin (specific for rods, Fig. 4 e-h) and cone transducin (specific for cones, Fig. 4 i-l) staining confirmed the finding and showed that the rod and cone outer segments faced correctly to the RPE in laminated transplants and faced the rosette center in rosetted transplants. There was no rhodopsin or cone transducin staining in the host (data not shown; see Figs. 1, 2 and 8 of (Seiler et al., 2017) indicating a complete loss of photoreceptor in the host at the time tested (5.8–8.6 months post surgery).

#### 3.3.2. Bipolar cells

To study the rod and cone bipolar cells, PKC $\alpha$  and secretagogin antibodies were used, respectively. As shown in Fig. 5, strong PKC $\alpha$ -positive rod bipolar cells were found in the host retina. Co-localization of PKC $\alpha$  and SC121 (human cytoplasmic marker) in transplants demonstrated that some donor progenitor cells developed into mature rod bipolar cells after the transplantation. In some areas, host rod bipolar cells extended processes into transplants (Fig. 5 d). Even in some transplants that only formed rosettes, the rosettes were very close to host rod bipolar cells and integrated with the host (Fig. 5 f,g).

Similarly, after the transplantation, some cells in the transplant developed into secretagogin-positive cone bipolar cells (Fig. 6). Compared with rod bipolar cells, there were much less cone bipolar cells in the transplant than in the host (Fig. 6 c and d). The transplant processes in the host IPL intermingled well with host cone bipolar cell processes (Fig. 6 e,f). Synaptophysin, marker for membrane protein of synaptic vesicles, also showed strong staining in both host and donor, indicating the good integration of host and donor tissues (Figs. 6 and 7).

#### 3.3.3. Human donor markers

Donor cellular processes and cells immunoreactive for SC121 (marker for cytoplasm of human cells) were found in the host retina (Figs. 4 and 5). To clarify whether donor cells migrate into the host retina, Ku80 (human nuclei marker) was used (Fig. 7 a-c, 8 c,d). As shown in Fig. 7 a, and 8 c, human retinal sheet transplants could form laminated structures, and some Ku80-positive (human nuclei marker) cells did migrate into host retina. H-E staining showed RPE in contact with transplant photoreceptors (Fig. 3 d, e and f). The cells were identified as RPE based on their location in the RPE layer and their pigmentation. In the same location on other sections nearby, these cells were Ku80-positive (Fig. 7 a, b) indicating they originated from human RPE of the donor. This was confirmed by CRALBP and Ku80 staining of adjacent sections (Supplementary Fig. 2).

#### 3.3.4. Transplant-host connectivity and synaptic markers

To examine synaptic connectivity between donor and host cells, a combination of SC121 and  $\alpha$ -synuclein (marker for rodent amacrine

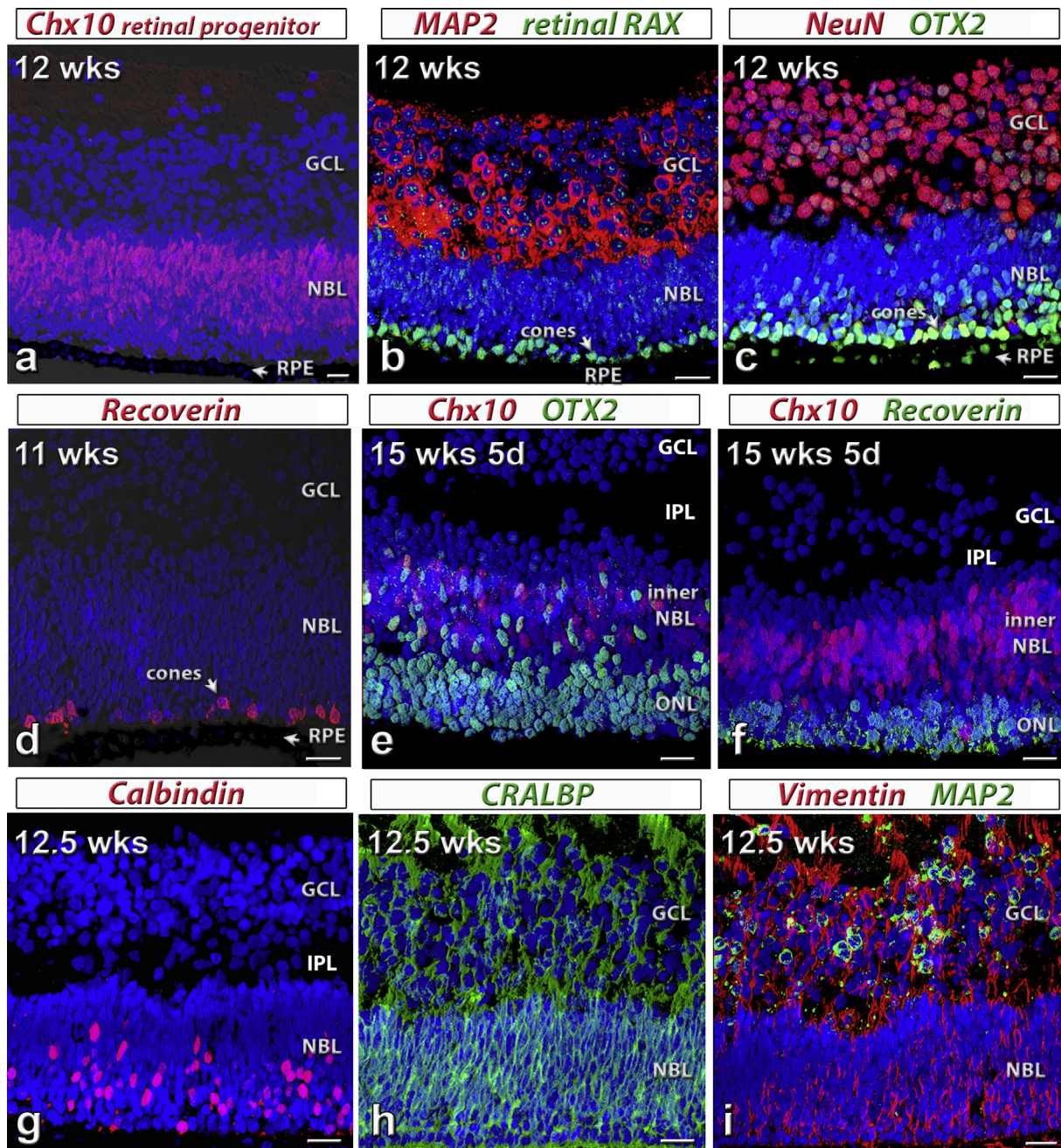


**Fig. 1.** Characterization of human fetal (HF) retina by immunohistochemistry. Nuclei are stained by DAPI (blue). (a)–(c): 12 weeks postconception. The retina contains a thick ganglion cell layer (GCL) and a neuroblastic layer (NBL). Arrow: retinal pigment epithelium (RPE). (a) Chx10 (red, retinal progenitor cell marker) in neuroblastic layer (NBL). (b) Cytoplasm of most cells in GCL: strongly label for MAP2 (microtubule-associated protein 2, red). Retinal RAX (retinal Homeobox protein, green): faint immunoreactivity in all nuclei; strong stain of nuclei of developing cones. (c) Intense NeuN (neuronal nuclei, red) stain of most ganglion cells. Strong OTX2 (Orthodenticle Homeobox 2, green) staining in RPE and developing photoreceptors. (d) 11 weeks postconception. Recoverin (red): scattered differentiating cone photoreceptors in NBL close to RPE. (e,f) 15 weeks 5 d postconception. The outer nuclear layer (ONL) has separated from the inner NBL. Retina has developed an inner plexiform layer (IPL). (e) Strong OTX2 (green) staining in developing photoreceptors and cells in inner NBL, some co-expressing Chx10 (red). (f) Recoverin (green) staining of several layers of developing photoreceptors. Chx10 (red) staining in inner NBL. (g–i) 12.5 weeks postconception. (g) Calbindin (red) staining of developing horizontal cells and cones in outer NBL. (h) CRALBP (cellular retinaldehyde protein, green) immunoreactivity of developing Müller cells. (i) Strong Vimentin (red) staining throughout. MAP2 (green) staining in GCL. Scale bars: 20  $\mu$ m. (For interpretation of the references to color in this figure legend, the reader is referred to the Web version of this article.)

cells and IPL) showed colocalization of both labels in the host IPL (Fig. 7 d,e). The addition of goat anti-synaptophysin (with a higher affinity for human) showed the SC121 (human),  $\alpha$ -Synuclein (rat) and Synaptophysin stained processes were seen in close contact to each other, suggesting that donor cells made synaptic connections with the host (Fig. 7 f,g). The synaptophysin marker showed clear IPL and OPL in the donor tissue but only IPL in the host retina (Figs. 6 and 7 a–c, f).

### 3.3.5. Glia and microglia

Several glial markers (GFAP, CRALBP) and microglia markers (Iba1 and CD68) were used to study glial and inflammatory responses to donor tissues in the host. In NIH nude rats with normal retina, GFAP + astrocytes were found on the retinal surface (optic fiber layer) and along blood vessels only (Fig. 8 a). More GFAP + glia were found in Müller cells of RD rats without surgery (data not shown) and sham

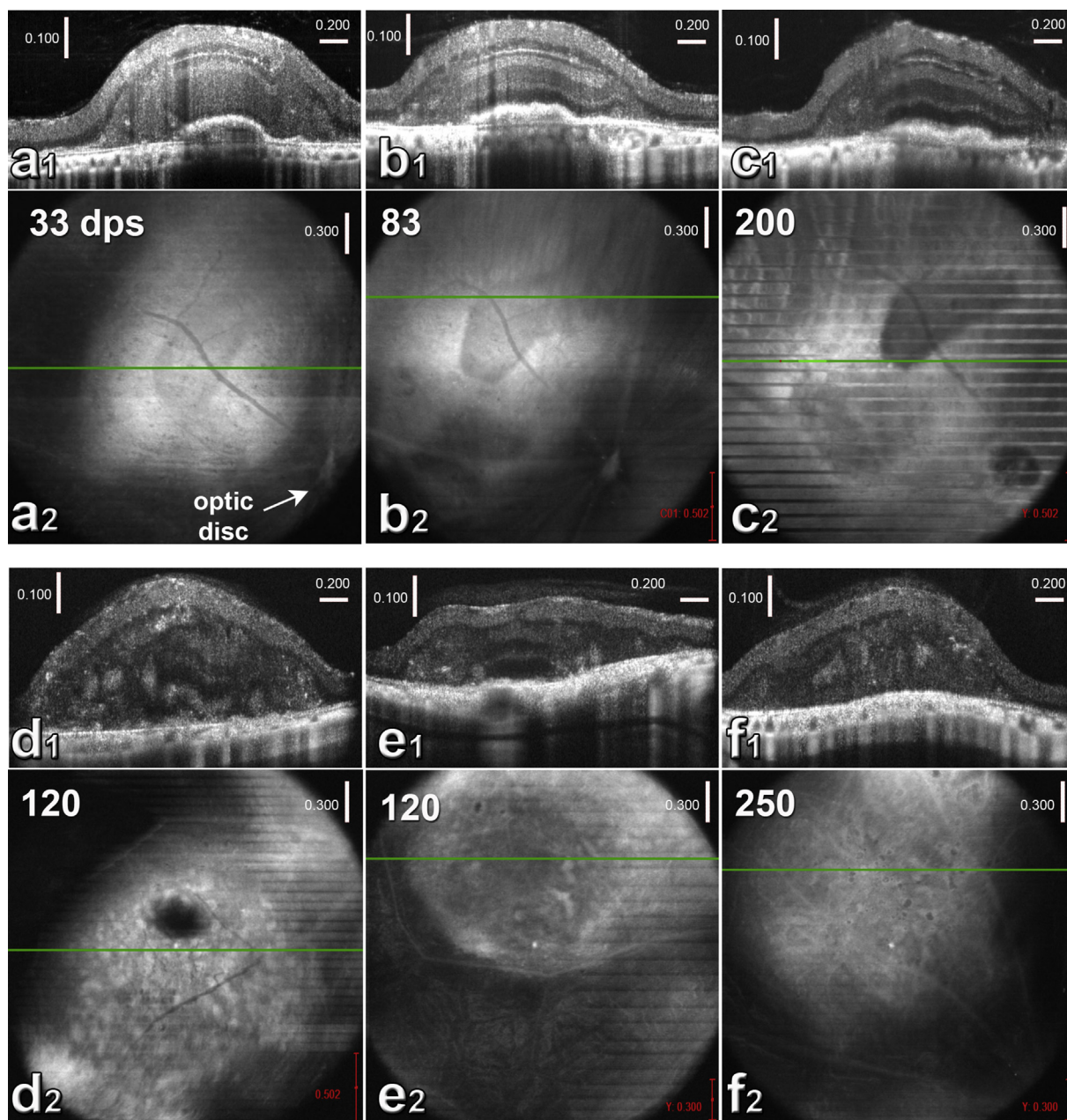


**Fig. 2.** OCT imaging of HF retinal transplants *in vivo*. (**a1**, **b1**, **c1**, **d1**, **e1**, **f1**): Cross-sectional B-scans. (**a2**, **b2**, **c2**, **d2**, **e2**, **f2**): corresponding fundus images (maximum projections). The green lines indicate the positions of the B-scans (above). (**a–c**) show the same transplant (rat #8) at different times post-transplantation. Dark area in the fundus image indicates cogenerated RPE. (**a1**) B-scan and (**a2**) fundus image at 33 day post-surgery (dps). At this time, only IPL and outer NBL of the transplant are recognizable in B-scan. (**b1**) B-scan and (**b2**) fundus image of the same eye at 83 dps. All retinal layers are visible in B-scan. (**c1**) B-scan and (**c2**) fundus image of the same eye at 200 dps. All retinal layers and outer segments are recognizable in B-scan. This fundus image is a narrower projection of the B-scans to show the RPE co-graft more clearly. Lines indicate rat breathing movements during scan. (**d1**) B-scan and (**d2**) fundus image of the eye of transplanted rat #7 at 120 dps. B-scan shows partial laminated structure in transplant. Rosettes are visible in both images (hyper-reflective spots). Optic disc is outside the fundus image. (**e1**) B-scan and (**e2**) fundus image of rat #9 at 120 dps. In B-scan, the center of the transplant appears laminated. Rosettes are recognizable too. (**f1**) B-scan and (**f2**) fundus images of rat #13 at 250 dps. Rosettes are visible. Scales in a1, b1, c1, d1, e1, and f1: vertical: 100  $\mu\text{m}$ ; horizontal: 200  $\mu\text{m}$ . Scales in a2, b2, c2, d2, e2, and f2: 300  $\mu\text{m}$ . (For interpretation of the references to color in this figure legend, the reader is referred to the Web version of this article.)

RD rats (Fig. 8 b) and in the host retina of transplanted RD rats (Fig. 8 c and d) likely due to retinal degeneration and injury caused by surgery. However, there was less GFAP-reactive glia in the donor tissue than in the host retina (Fig. 8 c and d). The CRALBP antibody labeled Müller cells and RPE. The intensity of CRALBP staining in NIH nude rats with normal retina (Fig. 8 e), sham RD rats (Fig. 8 f) and transplanted RD rats (Fig. 8 g, h; Supplementary Fig. 2) was similar. Müller cells were oriented radially in rosettes. Only few Iba1 stained microglia cells were found in IPL and OPL in the normal retina of NIH nude rats, which have

no T cells. Iba1 staining appeared to be similar in sham RD rats (Fig. 8 j) and transplanted RD rats (Fig. 8 k,l), indicating that there was no increase in microglia. CD68 + activated macrophages were found in sham RD rats (Fig. 8 j) and transplanted rats (Fig. 8 k and l) but mostly restricted to choroid. These data suggested that the donor tissue did not induce an inflammatory response after transplantation to this immunodeficient rat model.

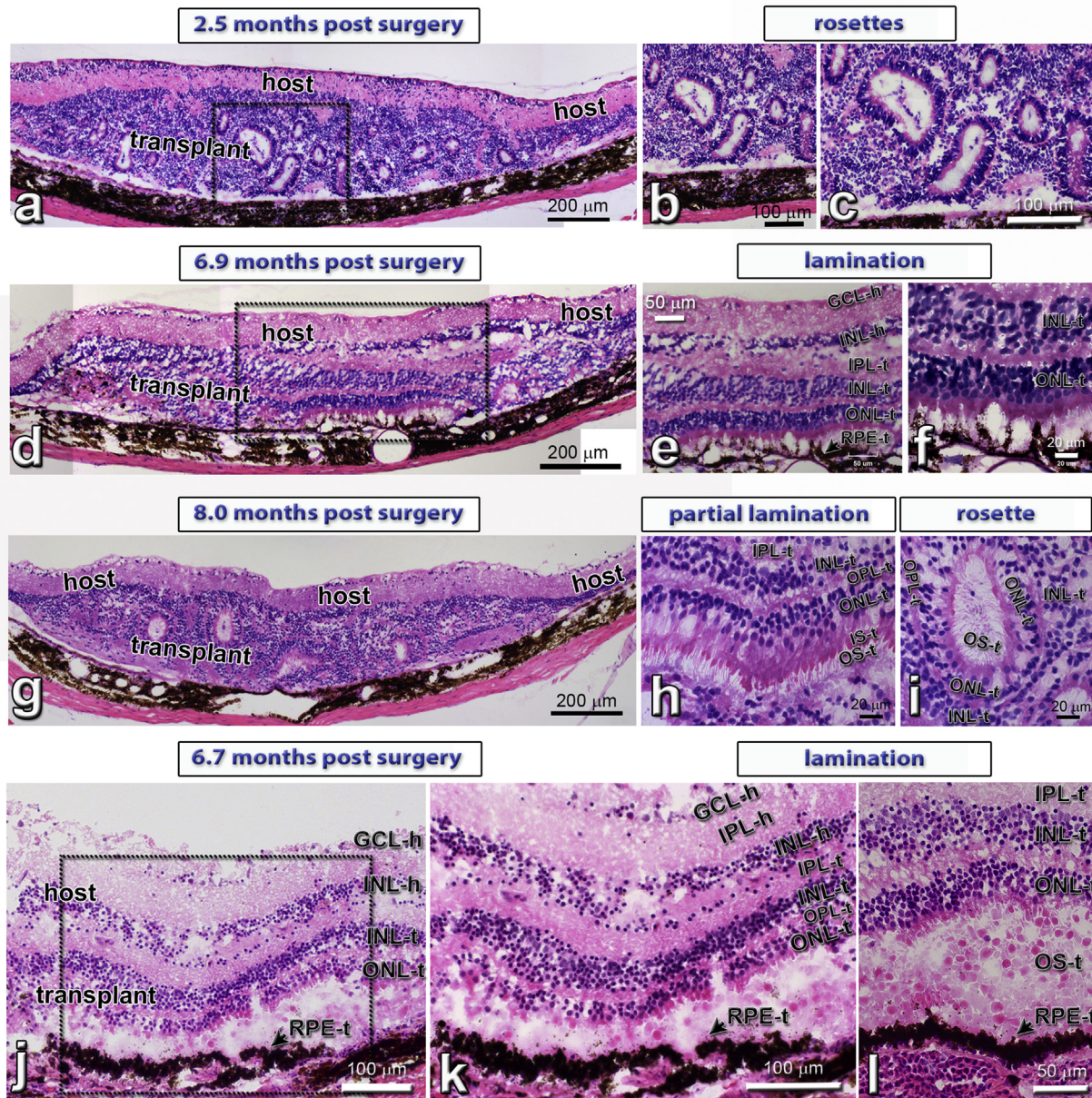


**Fig. 3.** Hematoxylin-Eosin (H-E) staining of HF retina transplants. (a–c): HF retina + RPE transplant, 2.5 months post surgery (rat #2): Formation of photoreceptors in rosettes, due to the difficult surgery in the rat eye. (d–f): HF retina + RPE transplant (#9), 6.9 months post surgery: lamination in transplant center with co-grafted RPE (see Fig. 7a b). Same transplant as in Fig. 2 e). (g–i): HF retinal transplant (#13), 8 months post surgery with partial lamination (h) and rosettes (i). Same transplant as in Fig. 2 f). (j–l): Laminated HF retina + RPE transplant (#8; same as in Fig. 2 a–c), 6.7 months after surgery. This rat was found dead overnight, therefore there are some postmortem artefacts. Scale bars are 200  $\mu\text{m}$  in (a, d, g), 100  $\mu\text{m}$  in (b, c, j, k), 50  $\mu\text{m}$  in (e, l) and 20  $\mu\text{m}$  (f, h, i). GCL = ganglion cell layer, IPL = inner plexiform layer, INL = inner nuclear layer, ONL = outer nuclear layer; RPE = retinal pigment epithelium; -h = host, -t = transplant.

### 3.4. Visual function improvement evaluated by superior colliculus (SC) electrophysiological recording

To access the visual improvement after transplantation, selected rats were analyzed by electrophysiological recording in the SC at 5.8–8.6 months after transplantation. Four of seven transplanted rats selected for SC electrophysiological recording showed responses to flashes of light (0.58 log cd/m<sup>2</sup>) in a limited area of SC after transplantation. In some rats, dimmer light (0.1 log cd/m<sup>2</sup>) could still evoke responses (Fig. 9, Table 3). In contrast, there was no response to flashes of light (0.58 log cd/m<sup>2</sup>) in age-matched sham surgery rats (n = 9, 3.3–8.9 MPS, age 4.2–9.9 months) or age matched control non-surgery rats (n = 12, age 4.5–9 months, Table 3).

### 4. Discussion

This is the first study evaluating the development of human fetal retinal sheets and their effect on visual function after transplantation into the RD nude rat model (*rho S334ter-3* rat), using OCT, immunohistochemistry and extracellular recordings in the superior colliculus. After transplantation, human retinal sheets survive long-term in an environment of advanced retinal degeneration, mature and develop into different retinal cells, integrate with the host retina, and improve visual function.

Previous work suggested that pre-differentiation of retinal stem cells to photoreceptors might be needed before they could integrate with the host retina (Canola et al., 2007). In the present study, human fetal retinas at 11–15.7 weeks gestation were used for transplantation. The cells were not mature although preliminary lamination had started to

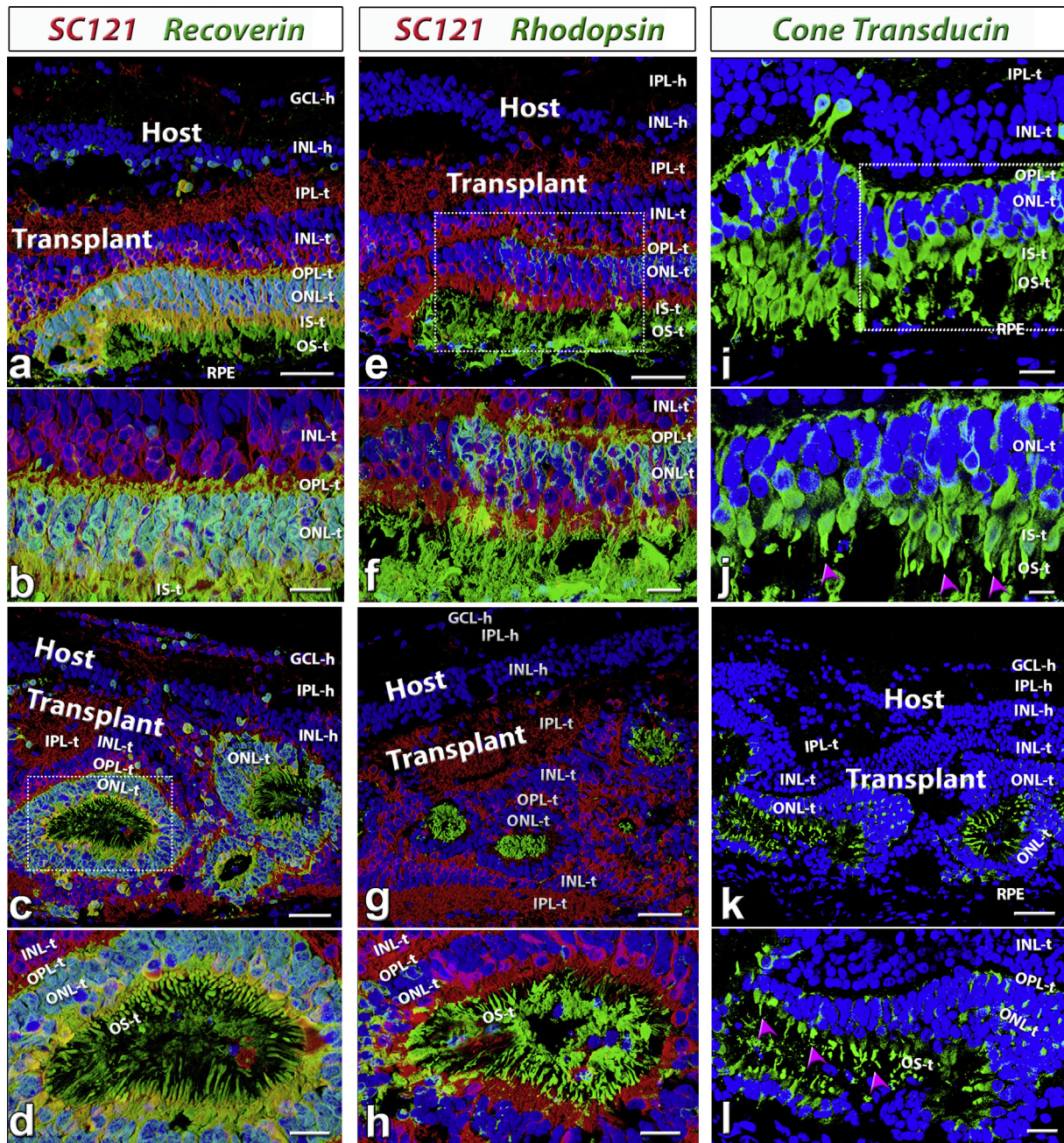


**Fig. 4.** Photoreceptor development in HF retina transplants. (a–d): Recoverin (photoreceptors and cone bipolar cells, green), SC121 (human cytoplasm, red). (e–h) Rhodopsin (rods, green), SC121 (red). (i–l): cone transducin (cones, green). Nuclei are stained blue (DAPI). (a,b,e,f,i,j) Laminated transplant (rat # 9) at 207 dps (same transplant as in Fig. 2 e; 3d). (a,b) Strong recoverin (green) labeling of photoreceptors and cone bipolar cells within the HFE transplant (red). Note that there is much fewer recoverin label in the host retina. (e,f) Transplant-specific rods. Strong staining of rod outer segments in transplant. There is no rhodopsin staining in host. (i, j) Transplant-specific cones in the outer nuclear layer of the transplant are correctly oriented with putative outer segments facing the RPE (purple arrow heads in (j)). (c,d,g,h,k,l): Many transplants however formed a rosetted morphology (rat #13; same transplant as in Fig. 2 f; 3g). Lamination within the rosettes of the transplant, however, was still apparent. Distinct outer nuclear, outer plexiform and inner nuclear layers surrounded the rosetted photoreceptors (c,d). Putative outer segments of rods (g,h) and cones (k, l; purple arrow heads) formed within the rosettes. Scale bars are 50  $\mu$ m in (a, c, e, g, k), 20  $\mu$ m in (b, d, f, h, i, l) and 10  $\mu$ m (j). GCL = ganglion cell layer, IPL = inner plexiform layer, INL = inner nuclear layer, ONL = outer nuclear layer; IS = inner segments, OS = outer segments, RPE = retinal pigment epithelium; -h = host, -t = transplant. (For interpretation of the references to color in this figure legend, the reader is referred to the Web version of this article.)

develop (Fig. 1). Thus, they had the plasticity to integrate with the host retina after transplantation, and were primed to differentiate into various retinal cell types, including photoreceptors.

The idea that fetal retinal sheets are the optimal transplants for cell replacement in advanced stage of retinal degenerate patients has been studied for many years. These sheets already contain a primordial circuitry and cells that are committed to differentiate into various retinal

cells (Seiler and Aramant, 2012). Our first published study of transplanted fetal retinal sheets was to a rat light damage model (Seiler and Aramant, 1998). Using a custom-made instrument and procedure, the sheets were gently placed into the subretinal space and later developed laminated layers of different cell types. Later, the same procedure was used to transplant rat fetal retina together with its RPE to RCS rats (Aramant et al., 1999) and human fetal retina with its RPE to athymic

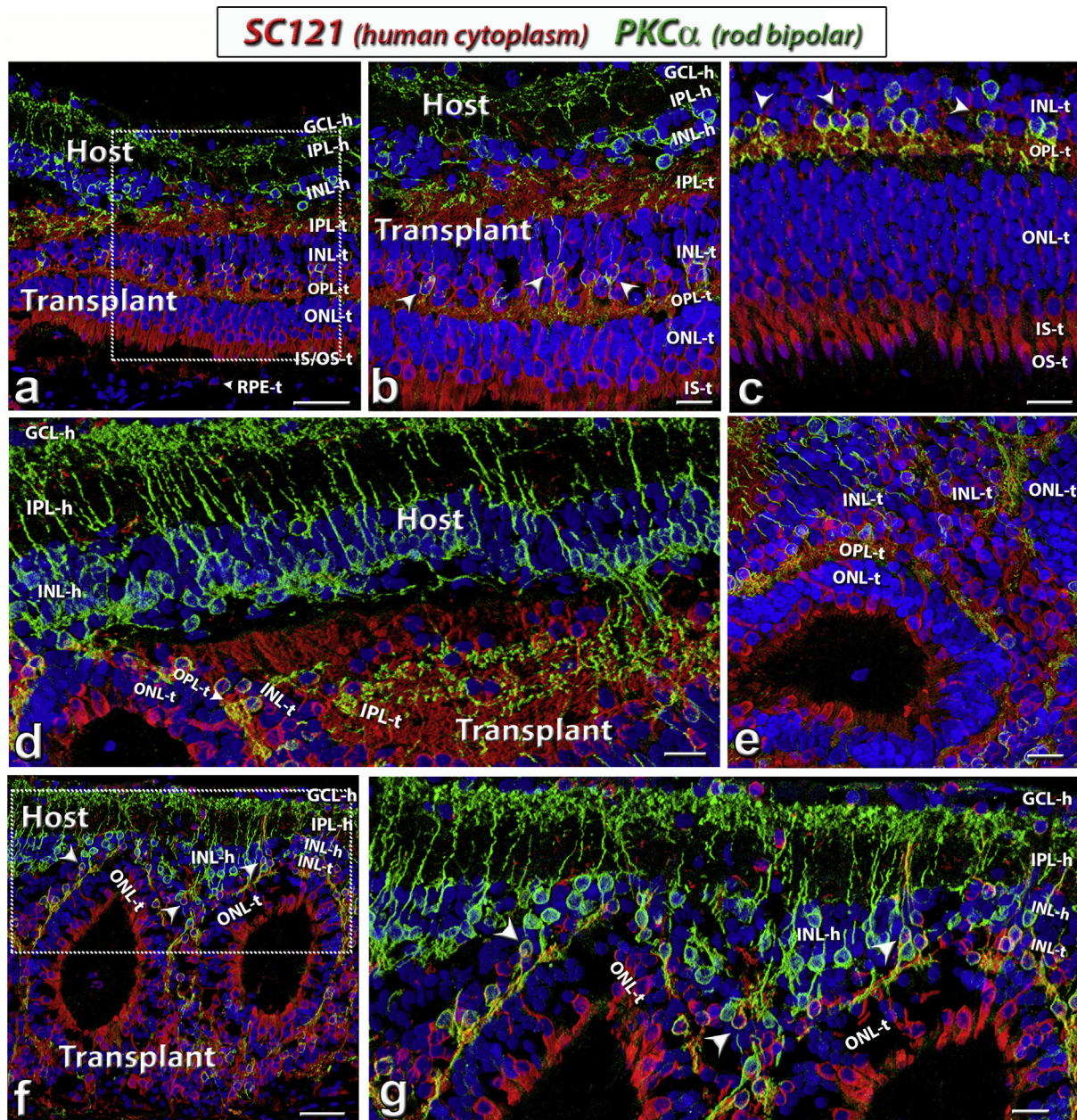


**Fig. 5.** Rod bipolar cells (PKC $\alpha$ ) development in HF retinal transplants. Combination of label for PKC $\alpha$  (protein kinase C  $\alpha$ ; rod bipolar cells, **green**), SC121 (human cytoplasm, **red**) and DAPI (cell nuclei, **blue**). (a–c): Well-laminated transplants in rat # 9 (a, b) and #12 (c). (d–g): Rosetted transplants in rat #7 (d, e) and #11 (f, g). Arrowheads point out co-localization of SC121 and PKC $\alpha$ , indicating donor rod bipolar cells. Donor and host tissues are well-integrated and in some areas, host rod bipolar cells extend processes into transplant (d). Scale bars are 50  $\mu$ m in (a, c, f) and 20  $\mu$ m in (b, d, e, g). GCL = ganglion cell layer, IPL = inner plexiform layer, INL = inner nuclear layer, OPL = outer plexiform layer, ONL = outer nuclear layer; IS = inner segments, OS = outer segments, RPE = retinal pigment epithelium; -h = host, -t = transplant. (For interpretation of the references to color in this figure legend, the reader is referred to the Web version of this article.)

nude rats (Aramant and Seiler, 2002b). Another group transplanted matrix-embedded human fetal neuroretina and RPE in a non-immunosuppressed minipig model of light-induced retinal degeneration (Li et al., 2009). The authors claimed that the transplants survived for up to 12 months, but rhodopsin-positive photoreceptor staining was not observed within the grafted tissue, which appeared degenerated. mfERG revealed some retinal functional improvement in regions both inside and outside of the grafted area.

In contrast, our unique transplantation method generated laminated retinal sheets that were well integrated with the host retina and improved visual function in several rat degeneration models (Woch et al., 2001; Sagdullaev et al., 2003; Thomas et al., 2004; Yang et al., 2010; Seiler et al., 2017).

Later, in a phase II clinical trial, sheets of human fetal retina transplants with RPE improved visual acuity in 7 of 10 patients (Radtke et al., 2008). The aim of the current study was to learn more about the mechanism of visual improvement with the same type of human transplant using an immunodeficient RD rat model. However, sub-retinal transplantation in the small rat eye with a large lens is more difficult than in the larger human eye where the surgeon can see and control the placement. Therefore, many transplants developed rosettes.

Comparable to the development of fetal retinal sheet transplantation in other groups (Ghosh et al., 1998, 2004; Ghosh and Arner, 2002; Bragadottir and Narfstrom, 2003), the transplants in the present study developed well laminated areas although rosettes were also present. Most mature retinal cells, including rod and cone photoreceptors, but

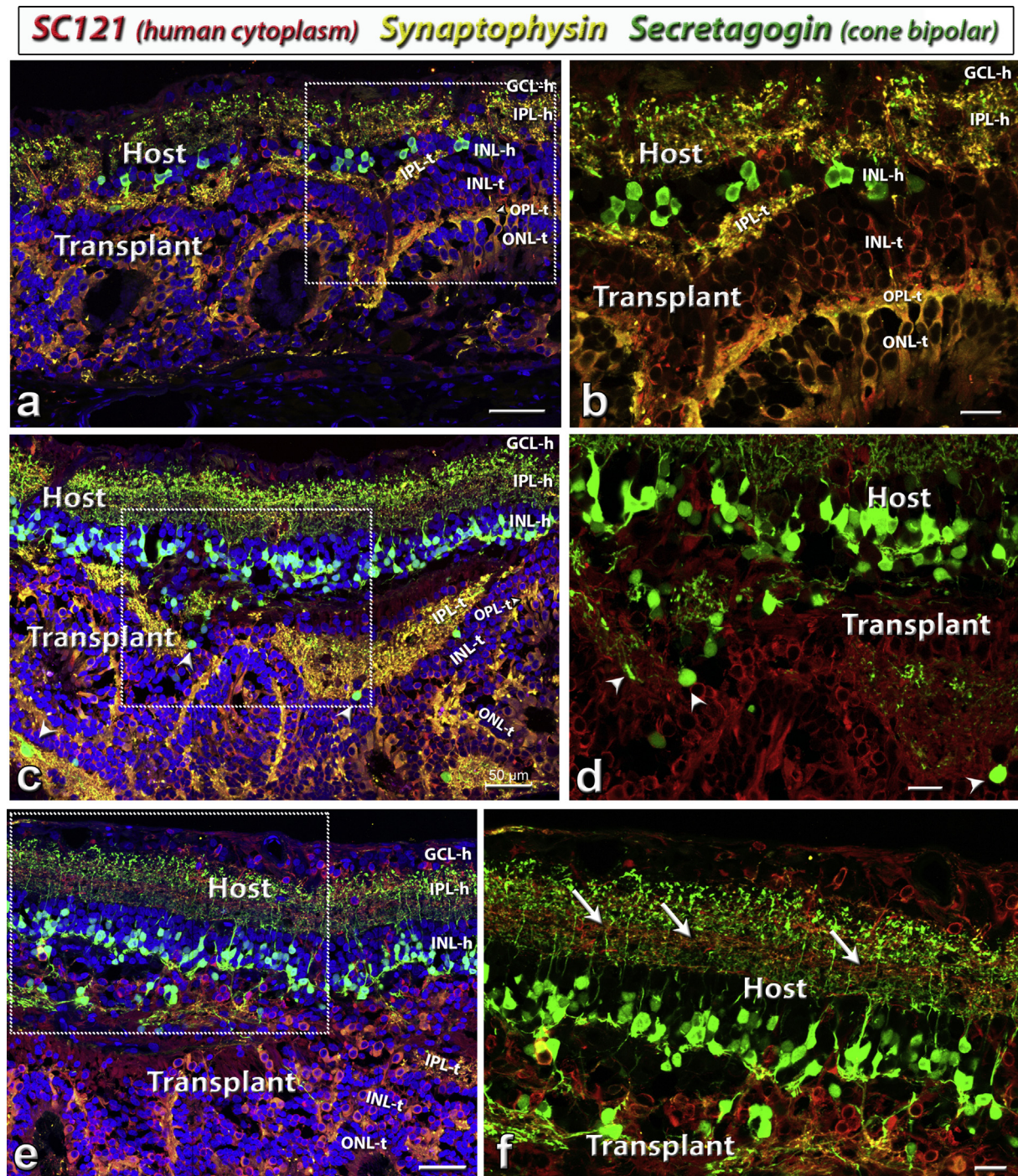


**Fig. 6.** Cone bipolar cells (Secretagogin) development in HF retinal transplants. Combination of label for Secretagogin (Cone bipolar cells, green), Synaptophysin (membrane protein of synaptic vesicles, goat antibody; yellow-gold), SC121 (human cytoplasm, red) and DAPI (cell nuclei, blue). Secretagogin labeling of cone bipolar cells in rat #9 (a, b) rat #13 (c, d,) and rat #6 (e, f). Most secretagogin-positive cone bipolar cells are found in the host but some are found in transplants (co-localization of secretagogin and SC121, arrow heads in (c, d). Many SC121 positive human cells have migrated into the host. Arrows in (f) point to SC121 labeled processes in host IPL. (b, d, f) are enlargement of the boxed area in (a, c, e) respectively. Scale bars are 50  $\mu\text{m}$  in (a, c, e) and 20  $\mu\text{m}$  in (b, d, f). GCL = ganglion cell layer, IPL = inner plexiform layer, INL = inner nuclear layer, OPL = outer plexiform layer, ONL = outer nuclear layer; -h = host, -t = transplant. (For interpretation of the references to color in this figure legend, the reader is referred to the Web version of this article.)

not ganglion cells, were found in the transplant. Donor processes labeled with the human cytoplasm marker SC121 were found in host retina, suggesting that the donor tissue fully integrated into the host. Recently, several groups found donor-host cytoplasmic exchange in the retina after transplantation of photoreceptor precursors, which required a re-evaluation of the mechanisms underlying rescue by photoreceptor transplantation (Pearson et al., 2016; Sanges et al., 2016; Santos-

Ferreira et al., 2016; Ortin-Martinez et al., 2017). To test if the donor cells do migrate into the host, we used Ku80, a human nuclear marker, and found many Ku80-stained cells in the host retina. Although we cannot exclude the possibility of cytoplasmic exchange (Pearson et al., 2016; Singh et al., 2016; Ortin-Martinez et al., 2017), our data did provide the proof of concept that transplanted human fetal retina tissue could migrate and integrate with the severely degenerated host retina.

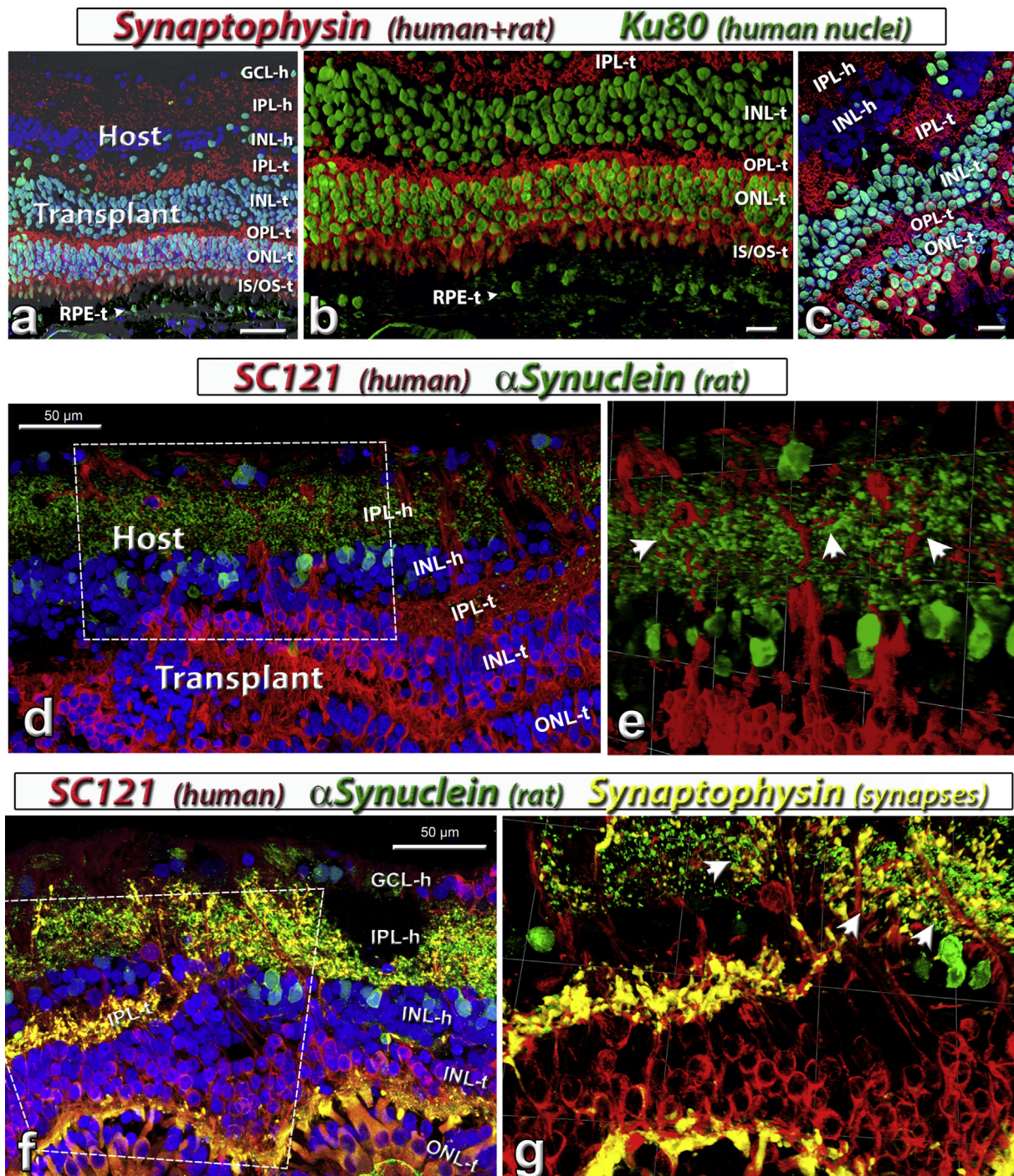


**Fig. 7.** Synaptic markers and connectivity in host and transplant. (a, b, c) Combination of label for synaptophysin (synaptic vesicles, mouse antibody; red), Ku80 (human nuclei, green) with DAPI (nuclei, blue). (a, b) Laminated transplant in rat #9. Synaptophysin staining of plexiform layers and cone inner segments. The image in (a) is in combination with brightfield and shows donor RPE (RPE-t) in interaction with transplant outer segments. Some transplant cells migrated into the host. (b) is enlargement of (a) without DAPI. (c) Rosetted transplant in rat #11. (d, e) Combination of SC121 (human cytoplasm, red) and  $\alpha$ -Synuclein (rodent amacrine cells and IPL, green) in rat #9. (e) is a tilted image created in Velocity ([www.cellularimaging.com](http://www.cellularimaging.com)) of the boxed area in (d), showing host IPL and transplant interface. Arrow heads point to the possible direct contact of host and transplant processes. (f, g) Combination of SC121 (human cytoplasm, red), synaptophysin (goat antibody, yellow-gold),  $\alpha$ -Synuclein (rodent amacrine cells and IPL, green) and DAPI (nuclei, blue) in rat #13. Strong synaptophysin staining of transplant inner plexiform (IPL-t) and outer plexiform layer (OPL-t). Note the extension of SC121-positive processes into the host IPL (IPL-h). (g) is a tilted image created in Velocity ([www.cellularimaging.com](http://www.cellularimaging.com)) of the boxed area in (f). Arrows point to possible synaptic contacts of host and transplant. Scale bars are 50  $\mu$ m in (a, d, f) and 20  $\mu$ m in (b, c, g). 1 unit in (e) equals 40.05  $\mu$ m, and 60.06  $\mu$ m in (g). GCL = ganglion cell layer, IPL = inner plexiform layer, INL = inner nuclear layer, OPL = outer plexiform layer, ONL = outer nuclear layer; -h = host, -t = transplant. (For interpretation of the references to color in this figure legend, the reader is referred to the Web version of this article.)

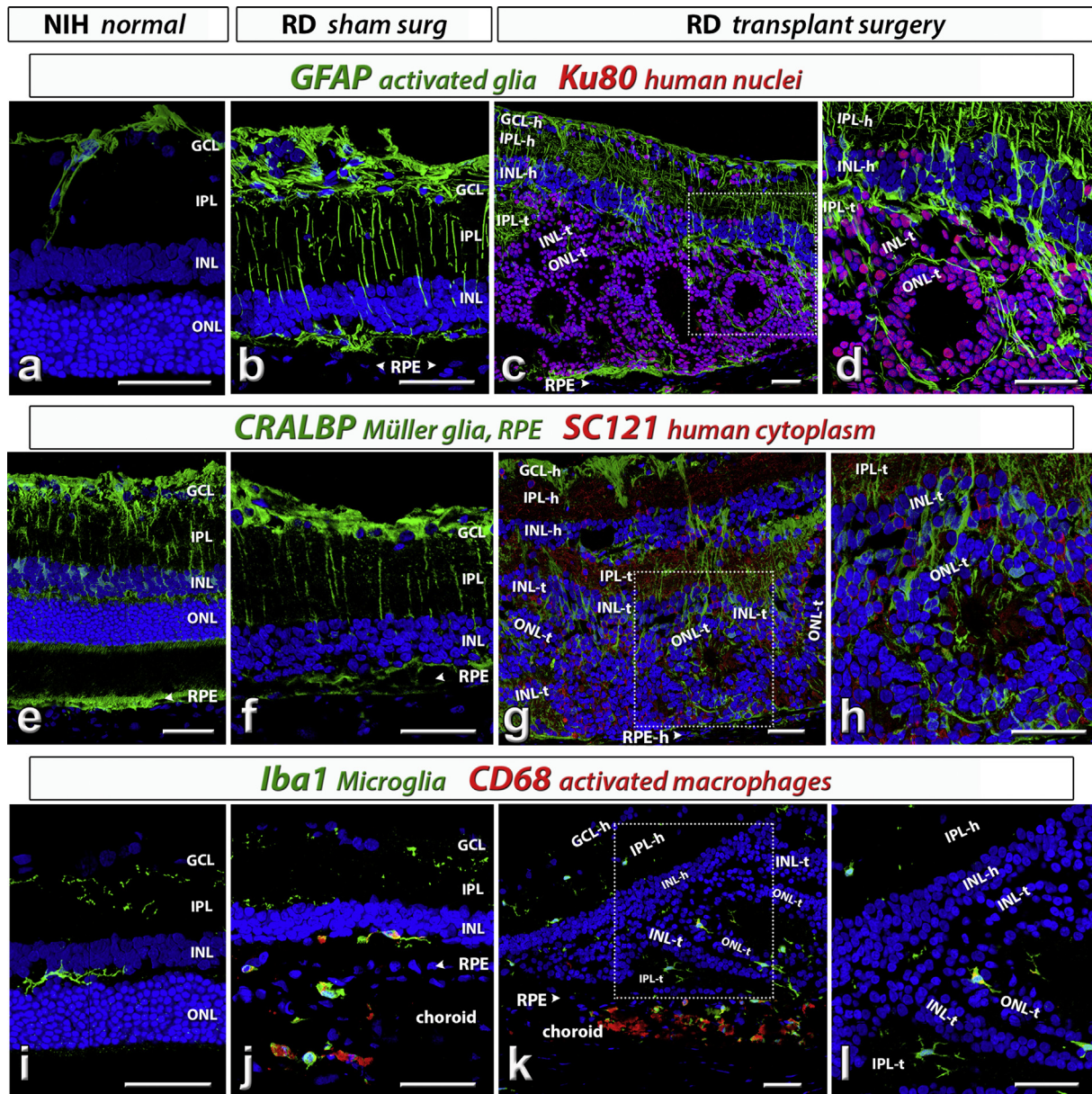


**Fig. 8.** Analysis of glia and microglia cells in host and transplant. (a–d) GFAP (glial fibrillary acidic protein, **green**). (a) In an NIH rat with normal retina, GFAP is only expressed in astrocytes on retinal surface and along blood vessels. (b) In a sham surgery RD rat, GFAP is also strongly expressed in Müller cells, in addition to astrocytes. (c,d) GFAP (**green**) and Ku80 (human nuclei, **red**) expression in a transplanted RD rat (#6). There is more GFAP staining in the retinal degenerate host than in transplant. Some donor cells have migrated into host retina. (e–h) CRALBP (cellular retinaldehyde binding protein, **green**). (e) CRALBP in Müller cells and RPE of a NIH rat with normal retina. (f) CRALBP expression in Müller cells and RPE of a sham surgery RD rat. (g,h) CRALBP and SC121 (human cytoplasm, **red**) staining in Müller cells and RPE of a transplanted RD rat (#13). Donor processes (SC121 +) extend into the host INL and IPL. The Müller cells in the transplant rosettes are radially oriented. (i–l) Iba1 (microglia, **green**) in combination with (j–l) CD68 (activated macrophages, **red**). (i) Microglia in IPL and OPL of a NIH rat with normal retina. (j) microglia (**green**) and activated macrophages (**red**) staining in a sham surgery RD rat. Microglia are mainly observed in IPL and subretinal space; while activated macrophages are mainly found in the choroid. (k,l) Iba1 (**green**) and CD68 (**red**) staining in a transplanted RD rat (#13). Iba1 + microglia are seen in both host and donor and CD68 + cells were mostly restricted to the choroid and not found in the transplant. (d), (h) and (l) were enlargement of the boxed area in (c), (g) and (k) respectively. Scale bars: 50  $\mu$ m. GCL = ganglion cell layer, IPL = inner plexiform layer, INL = inner nuclear layer, ONL = outer nuclear layer; -h = host, -t = transplant. (For interpretation of the references to color in this figure legend, the reader is referred to the Web version of this article.)

Interestingly, our previous work showed that although rat fetal donor retina fully integrated with the same RD rat host, the donor tissue stayed in the subretinal space and did not migrate much into the host retina; but in the present study, the human donor cells migrated into the host retina to a large extent. These results suggest that human fetal retina, transplanted at an earlier developmental stage, may have a larger migration potential than the more mature transplanted rat fetal tissue. These results may shed some light on the mechanism of the increased retinal sensitivity not only in the transplant area but also in the

adjacent area in the phase II clinical trial (Radtke et al., 2008). However, since the retinal transplants were often seen to enlarge in size, migrate into the adjacent area after the transplantation and improve vision, it cannot be excluded that some trophic effect might also contribute.

Although the outer limiting membrane of the Müller cells in a degenerating retina has been considered an obstacle for transplant integration (Hippert et al., 2016), this does not appear to be the case with human fetal retinal sheets. Staining for glial markers indicated

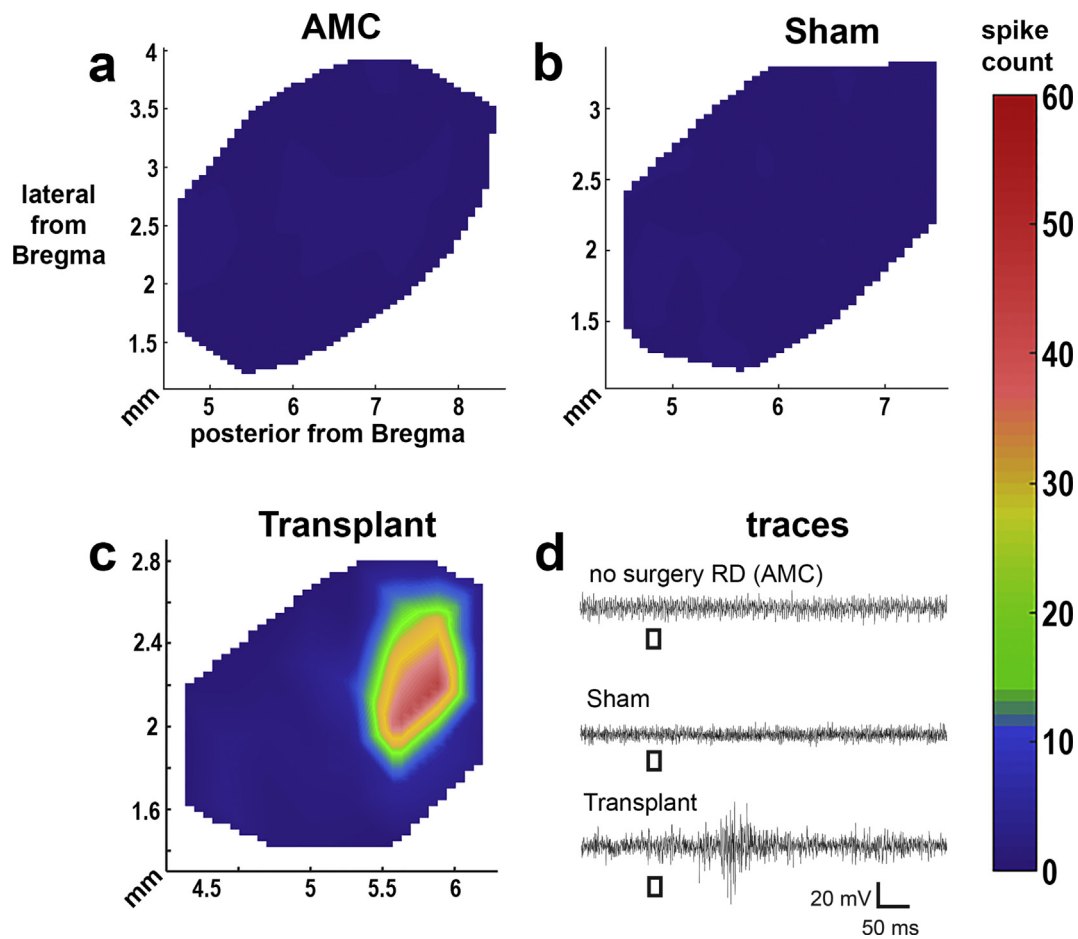


**Fig. 9.** Visual improvement assessed by superior colliculus (SC) recording. Representative spike count heatmaps of (a) non-surgery age matched control (AMC), (b) sham surgery, and (c) transplanted rat with response (#13). No response was found in the entire SC area of non-surgery AMC and sham rats. Strong responses were found in some areas of the SC in 4 of 7 recorded transplant rats (see Table 3). (d) Traces are representative from either the location with the strongest response in transplant rats or a random location in non-surgery AMC and sham rat. The scale bar applies to all traces and the color bar applies to all heatmaps. (For interpretation of the references to color in this figure legend, the reader is referred to the Web version of this article.)

activation of Müller glia in the RD retina due to the photoreceptor degeneration, but much less GFAP staining in the transplant. The number of microglia cells appeared to be unchanged after transplantation. This indicated the absence of an inflammatory response in the immunodeficient host retina to the human xenograft.

Another interesting observation in this study: the vision improvements with human transplants were weaker than those found with rat transplants in the same RD rat model (Seiler et al., 2017). Two of the reasons might be (1) the different development time of rat versus human cells, since at the time of recording, the human photoreceptors had not yet matured to the same extent as the rat cells; (2) more

difficulty in development and synaptic formation of xenotransplantation (human to rat) compared with allotransplantation (rat to rat). Our result is consistent with the report of another lab showing less vision improvement of hESC retina transplants compared with miPSC retina in NOG-rd1-2J mice (Iraha et al., 2018).

In the past decade, following the findings that stem cells, such as hESCs and iPSCs, can be differentiated into 3 D retinal organoids comparable to fetal retina (Osakada et al., 2009; La Torre et al., 2012; Mellough et al., 2012; Nakano et al., 2012; Zhong et al., 2014), stem cells have been considered a promising source of cell therapy for retinal diseases and attract more and more interests. Stem cell-derived RPE

**Table 3**  
Summary of SC data of human fetal retinal (HFR) transplants, and compared with that of rat fetal retinal transplants.

	Rat ID	Donor age	Age at surgery (d)	Age at recording (d)	Time post-surgery (d)	% responsive/recorded area	Max spike count	Best response threshold (log cd/m <sup>2</sup> )
HFR transplants	5	11 wk 1 day	26	199	173	8	24.2	0.36
	6	11 wk 1 day	26	229	203	10.20	19.0	0.36
	9	11 wk 3 day	31	238	207	6.67	11.5	0.58
	13	11 wk 5 days	27	284	257	31.43	51.7	0.10
	Mean		27.50	237.50	210.00	14.07	26.6	0.35
	SEM	1.19	17.60	17.41	5.05	7.6	0.08	
rat <sup>a</sup> transplants	Mean		31.6	191.38	159.13	19.75	50.05	-0.13
	SEM		1.78	22.27	24.19	6.23	10.93	0.40

<sup>a</sup> Summary of the data in previous work (Seiler et al., 2017).

cells were successfully transplanted into the eyes of RD animal models and patients in phase I/II studies, and showed function improvement (Schwartz et al., 2015, 2016; Koss et al., 2016; Peng et al., 2016). After transplantation into the eyes of RD animal models, hESC/iPSC-derived photoreceptor precursors could develop into mature photoreceptors, integrate with the host, and improve visual function (Assawachananont et al., 2014; Shirai et al., 2016; Iraha et al., 2018). Because of the difference in animal model and methods for functional testing, it is hard to compare their data with our current results. Recently, we transplanted hESC-derived retinal organoid sheets to the same RD rat model and found qualitatively better vision improvement than with human fetal retinal transplants (McLelland et al., in press). It may be attributed to (1) fetal retinas were harvested at least one day before transplantation and shipped overnight in hibernate E medium on ice, while hESC-derived retinal organoids could be used right after being taken from the incubator; (2) hESC-derived retinal organoids may be more immature than fetal retina so that they have better potential to survive in the host. Two advantages of fetal retinal transplants were noticed: (1) they never grew into tumors, maybe because the cells were committed to differentiate into mature retinal cells; (2) they develop into laminated layers similar to normal retinal structure while stem cell-derived retinal cells formed only rosettes but not parallel laminated layers in all the studies so far (Iraha et al., 2018; McLelland et al., in press). More studies are needed to optimize stem cell transplants before they could be used in RD patients as a regular therapy.

## 5. Conclusions

This study demonstrates that transplanted human fetal retinal sheets continue to develop and differentiate into mature retinal cells in a severely degenerative environment and improve vision by direct connection with the host retinal circuitry. The findings provide significant insight for using fetal retinal sheet transplantation as a therapeutic strategy to restore vision after severe retinal degeneration. Ethically obtained fetal retinas can potentially be used to improve vision of RD patients while other methods such as stem cell transplants are still under development.

## Funding

Supported by CIRM TR4-06648; Lincy Foundation.

## Commercial relationships disclosure

MJS and RBA have a proprietary interest in the implantation instruments and method.

## Acknowledgements

The authors wish to thank Fengrong Yan, Lakshmi Patil (technical assistance); Alexander de Guzman (OCT), Navjot Kaur, Jacson Wan, Parth Patel, Mony Sary (cryostat cutting and staining); Robert Lin, Ph.D. (SC recording); Brian Cummings, Ph.D. (help and support); Hans S. Keirstead (HSK), Ph.D. (previously UC Irvine; now AIVITA Biomedical Inc., support), Biju B. Thomas, Ph.D. (USC, Dept. Ophthalmology, advice, training and support). Supported by CIRM TR4-06648 (MJS), and NIH grant R01EY024045 (HSK). A grant of the Lincy foundation (LF-42108) (HSK) provided support previously for obtaining fetal tissue for immunohistochemical analysis.

## Appendix A. Supplementary data

Supplementary data related to this article can be found at <http://dx.doi.org/10.1016/j.exer.2018.05.017>.

## List of abbreviations in text and figures

DAPI	4,6-diamidinodiamidino-2-phenylindole
AMC	age-matched control
BM	Bruch's membrane
CRALBP	cellular retinaldehyde binding protein
dps	days post-surgery
DAB	diaminobenzidine
GCL	ganglion cell layer
GFAP	glial fibrillary acidic protein
H&E	hematoxylin and eosin
-h	host
HFR	human fetal retina
INL	inner nuclear layer
IPL	inner plexiform layer
IS	inner segments
Iba-1	ionized calcium binding adaptor molecule 1
MAP2	microtubule-associated protein 2
MPS	months post-surgery
NBL	neuroblastic layer
NeuN	neuronal nuclei
OLM	Outer limiting membrane
OTX2	orthodenticle homeobox 2
ONL	outer nuclear layer
OPL	outer plexiform layer
OS	outer segments
PBS	phosphate buffered saline
PKC $\alpha$	protein kinase C $\alpha$
RD	retinal degenerate; retinal degeneration
RPE	retinal pigment epithelium
SD-OCT	spectral-domain optical coherence tomography
SC121	stem cell 121 antibody
SC	superior colliculus
-t	transplant
wks	weeks

## References

- Anderson, A.J., Haus, D.L., Hooshmand, M.J., Perez, H., Sontag, C.J., Cummings, B.J., 2011. Achieving stable human stem cell engraftment and survival in the CNS: is the future of regenerative medicine immunodeficient? *Regen. Med.* 6, 367–406 PubMed ID 21548741.
- Aramant, R.B., Seiler, M.J., 2002a. Retinal transplantation—advantages of intact fetal sheets. *Prog. Retin. Eye Res.* 21, 57–73 PubMed ID 11906811.
- Aramant, R.B., Seiler, M.J., 2002b. Transplanted sheets of human retina and retinal pigment epithelium develop normally in nude rats. *Exp. Eye Res.* 75, 115–125 PubMed ID 12137757.
- Aramant, R.B., Seiler, M.J., Ball, S.L., 1999. Successful cotransplantation of intact sheets of fetal retina with retinal pigment epithelium. *Invest. Ophthalmol. Vis. Sci.* 40, 1557–1564 PubMed ID 10359338.
- Assawachananont, J., Mandai, M., Okamoto, S., Yamada, C., Eiraku, M., Yonemura, S., Sasai, Y., Takahashi, M., 2014. Transplantation of embryonic and induced pluripotent stem cell-derived 3D retinal sheets into retinal degenerative mice. *Stem cell reports* 2, 662–674 PubMed ID 24936453.
- Bennett, J., Tanabe, T., Sun, D., Zeng, Y., Kjeldbye, H., Gouras, P., Maguire, A.M., 1996. Photoreceptor cell rescue in retinal degeneration (rd) mice by in vivo gene therapy. *Nat. Med.* 2, 649–654 PubMed ID 8640555.
- Bragadottir, R., Narfstrom, K., 2003. Lens sparing pars plana vitrectomy and retinal transplantation in cats. *Vet. Ophthalmol.* 6, 135–139 PubMed ID 12753615.
- Brundin, P., Barbin, G., Strecker, R.E., Isacson, O., Prochiantz, A., Bjorklund, A., 1988. Survival and function of dissociated rat dopamine neurons grafted at different developmental stages or after being cultured in vitro. *Brain Res.* 467, 233–243 PubMed ID 3378172.
- Canola, K., Angenieux, B., Tekaya, M., Quiambao, A., Naash, M.I., Munier, F.L., Schorderet, D.F., Arsenijevic, Y., 2007. Retinal stem cells transplanted into models of late stages of retinitis pigmentosa preferentially adopt a glial or a retinal ganglion cell fate. *Invest. Ophthalmol. Vis. Sci.* 48, 446–454 PubMed ID 17197566.
- Cibulskite, D., Kaalund, H., Pedersen, M., Horlyck, A., Marcussen, N., Hansen, H.E., Madsen, M., Mortensen, J., 2005. Chronic cyclosporine nephrotoxicity: a pig model. *Transplant. Proc.* 37, 3298–3301 PubMed ID 16298579.
- Cooper, A.E., Cho, J.H., Menges, S., Masood, S., Xie, J., Yang, J., Klassen, H., 2016. Immunosuppressive treatment can alter visual performance in the royal college of surgeons rat. *J. Ocul. Pharmacol. Therapeut.* 32, 296–303 PubMed ID 27008099.
- de Jong, P.T., 2006. Age-related macular degeneration. *N. Engl. J. Med.* 355, 1474–1485

- PubMed ID 17021323.
- Dizhoor, A.M., Ray, S., Kumar, S., Niemi, G., Spencer, M., Brolley, D., Walsh, K.A., Philipov, P.P., Hurley, J.B., Stryer, L., 1991. Recoverin: a calcium sensitive activator of retinal rod guanylate cyclase. *Science* 251, 915–918 PubMed ID 1672047.
- Ghosh, F., Arner, K., 2002. Transplantation of full-thickness retina in the normal porcine eye: surgical and morphologic aspects. *Retina* 22, 478–486 PubMed ID 12172116.
- Ghosh, F., Arner, K., Ehinger, B., 1998. Transplant of full-thickness embryonic rabbit retina using pars plana vitrectomy. *Retina* 18, 136–142 PubMed ID 9564694.
- Ghosh, F., Johansson, K., Ehinger, B., 1999. Long-term full-thickness embryonic rabbit retinal transplants. *Invest. Ophthalmol. Vis. Sci.* 40, 133–142 PubMed ID 9888436.
- Ghosh, F., Wong, F., Johansson, K., Bruun, A., Petters, R.M., 2004. Transplantation of full-thickness retina in the rhodopsin transgenic pig. *Retina* 24, 98–109 PubMed ID 15076950.
- Gouras, P., Tanabe, T., 2003. Survival and integration of neural retinal transplants in rd mice. *Graefes Arch. Clin. Exp. Ophthalmol.* 241, 403–409 PubMed ID 12698256.
- Hanus, J., Zhao, F., Wang, S., 2016. Current therapeutic developments in atrophic age-related macular degeneration. *Br. J. Ophthalmol.* 100, 122–127 PubMed ID 26553922.
- Hartong, D.T., Berson, E.L., Dryja, T.P., 2006. Retinitis pigmentosa. *Lancet* 368, 1795–1809 PubMed ID 17113430.
- Hippert, C., Graca, A.B., Pearson, R.A., 2016. Gliosis can impede integration following photoreceptor transplantation into the diseased retina. *Adv. Exp. Med. Biol.* 854, 579–585 PubMed ID 26427462.
- Hoshino, A., Ratnapriya, R., Brooks, M.J., Chaitankar, V., Wilken, M.S., Zhang, C., Starostik, M.R., Gieser, L., La Torre, A., Nishio, M., Bates, O., Walton, A., Bermingham-McDonogh, O., Glass, I.A., Wong, R.O.L., Swaroop, A., Reh, T.A., 2017. Molecular anatomy of the developing human retina. *Dev. Cell* 43, 763–779 e764. PubMed ID 29233477.
- Huang, R., Baranov, P., Lai, K., Zhang, X., Ge, J., Young, M.J., 2014. Functional and morphological analysis of the subretinal injection of human retinal progenitor cells under Cyclosporin A treatment. *Mol. Vis.* 20, 1271–1280 PubMed ID 25352736.
- Iraha, S., Tu, H.Y., Yamasaki, S., Kagawa, T., Goto, M., Takahashi, R., Watanabe, T., Sugita, S., Yonemura, S., Sunagawa, G.A., Matsuyama, T., Fujii, M., Kuwahara, A., Kishino, A., Koide, N., Eiraku, M., Tanihara, H., Takahashi, M., Mandai, M., 2018. Establishment of immunodeficient retinal degeneration model mice and functional maturation of human ESC-derived retinal sheets after transplantation. *Stem cell reports* 10, 1059–1074 PubMed ID 29503091.
- Ivert, L., Gouras, P., Naeser, P., Narfstrom, K., 1998. Photoreceptor allografts in a feline model of retinal degeneration. *Graefes Arch. Clin. Exp. Ophthalmol.* 236, 844–852 PubMed ID 9825260.
- Juliusson, B., Bergstrom, A., van Veen, T., Ehinger, B., 1993. Cellular organization in retinal transplants using cell suspensions or fragments of embryonic retinal tissue. *Cell Transplant.* 2, 411–418 PubMed ID 8162282.
- Koss, M.J., Falabella, P., Stefanini, F.R., Pfister, M., Thomas, B.B., Kashani, A.H., Brant, R., Zhu, D., Clegg, D.O., Hinton, D.R., Humayun, M.S., 2016. Subretinal implantation of a monolayer of human embryonic stem cell-derived retinal pigment epithelium: a feasibility and safety study in Yucatan minipigs. *Graefes Arch. Clin. Exp. Ophthalmol.* 254, 1553–1565 PubMed ID 27335025.
- La Torre, A., Lamba, D.A., Jayabalu, A., Reh, T.A., 2012. Production and transplantation of retinal cells from human and mouse embryonic stem cells. *Meth. Mol. Biol.* 884, 229–246 PubMed ID 22688710.
- LaVail, M.M., 2005. Survival factors for treatment of retinal degenerative disorders: preclinical gains and issues for translation into clinical studies. *Retina* 25, S25–S26 PubMed ID 16374321.
- Li, S.Y., Yin, Z.Q., Chen, S.J., Chen, L.F., Liu, Y., 2009. Rescue from light-induced retinal degeneration by human fetal retinal transplantation in minipigs. *Curr. Eye Res.* 34, 523–535 PubMed ID 19899965.
- Lindvall, O., Bjorklund, A., 2011. Cell therapeutics in Parkinson's disease. *Neurotherapeutics* 8, 539–548 PubMed ID 21901584.
- Liu, M.M., Tuo, J., Chan, C.C., 2011. Gene therapy for ocular diseases. *Br. J. Ophthalmol.* 95, 604–612 PubMed ID 20733027.
- MacLaren, R.E., Pearson, R.A., MacNeil, A., Douglas, R.H., Salt, T.E., Akimoto, M., Swaroop, A., Sowden, J.C., Ali, R.R., 2006. Retinal repair by transplantation of photoreceptor precursors. *Nature* 444, 203–207 PubMed ID 17093405.
- Mansergh, F.C., Vawda, R., Millington-Ward, S., Kenna, P.F., Haas, J., Gallagher, C., Wilson, J.H., Humphries, P., Ader, M., Farrar, G.J., 2010. Loss of photoreceptor potential from retinal progenitor cell cultures, despite improvements in survival. *Exp. Eye Res.* 91, 500–512 PubMed ID 20637750.
- McLelland, B.T., Lin, B., Mathur, A., Aramant, R.B., Thomas, B.B., Nistor, G., Keirstead, H.S., Seiler, M.J., (in press). Transplanted hESC-retina organoid sheets differentiate, integrate and improve visual function in retinal degenerate rats. *Invest Ophthalmol Vis Sci.* 59. <https://doi.org/10.1167/iov.17-23646>.
- Medeiros, N.E., Curcio, C.A., 2001. Preservation of ganglion cell layer neurons in age-related macular degeneration. *Invest. Ophthalmol. Vis. Sci.* 42, 795–803 PubMed ID 11222543.
- Mellough, C.B., Sernagor, E., Moreno-Gimeno, I., Steel, D.H., Lako, M., 2012. Efficient stage-specific differentiation of human pluripotent stem cells toward retinal photoreceptor cells. *Stem cells (Dayton, Ohio)* 30, 673–686 PubMed ID 22267304.
- Molday, R.S., MacKenzie, D., 1983. Monoclonal antibodies to rhodopsin: characterization, cross-reactivity, and application as structural probes. *Biochemistry* 22, 653–660 PubMed ID 6188482.
- Nakano, T., Ando, S., Takata, N., Kawada, M., Muguruma, K., Sekiguchi, K., Saito, K., Yonemura, S., Eiraku, M., Sasai, Y., 2012. Self-formation of optic cups and storable stratified neural retina from human ESCs. *Cell Stem Cell* 10, 771–785 PubMed ID 22704518.
- O'Brien, K.M., Schulte, D., Hendrickson, A.E., 2003. Expression of photoreceptor-associated molecules during human fetal eye development. *Mol. Vis.* 9, 401–409 PubMed ID 12949469.
- Ortin-Martinez, A., Tsai, E.L., Nickerson, P.E., Bergeret, M., Lu, Y., Smiley, S., Comanita, L., Wallace, V.A., 2017. A reinterpretation of cell transplantation: GFP transfer from donor to host photoreceptors. *Stem cells (Dayton, Ohio)* 35, 932–939 PubMed ID 27977075.
- Osakada, F., Ikeda, H., Sasai, Y., Takahashi, M., 2009. Stepwise differentiation of pluripotent stem cells into retinal cells. *Nat. Protoc.* 4, 811–824 PubMed ID 19444239.
- Pearson, R.A., Barber, A.C., Rizzi, M., Hippert, C., Xue, T., West, E.L., Duran, Y., Smith, A.J., Chuang, J.Z., Azam, S.A., Luhmann, U.F., Benucci, A., Sung, C.H., Bainbridge, J.W., Carandini, M., Yau, K.W., Sowden, J.C., Ali, R.R., 2012. Restoration of vision after transplantation of photoreceptors. *Nature* 485, 99–103 PubMed ID 22522934.
- Pearson, R.A., Barber, A.C., West, E.L., MacLaren, R.E., Duran, Y., Bainbridge, J.W., Sowden, J.C., Ali, R.R., 2010. Targeted disruption of outer limiting membrane junctional proteins (Crb1 and ZO-1) increases integration of transplanted photoreceptor precursors into the adult wild-type and degenerating retina. *Cell Transplant.* 19, 487–503 PubMed ID 20089206.
- Pearson, R.A., Gonzalez-Cordero, A., West, E.L., Ribeiro, J.R., Aghaizu, N., Goh, D., Sampson, R.D., Georgiadis, A., Waldron, P.V., Duran, Y., Naeem, A., Kloc, M., Cristante, E., Kruczek, K., Warre-Cornish, J.C., Sowden, J.C., Smith, A.J., Ali, R.R., 2016. Donor and host photoreceptors engage in material transfer following transplantation of post-mitotic photoreceptor precursors. *Nat. Commun.* 7, 13029 PubMed ID 27701378.
- Peng, C.H., Chuang, J.H., Wang, M.L., Jhan, Y.Y., Chien, K.H., Chung, Y.C., Hung, K.H., Chang, C.C., Lee, C.K., Tseng, W.L., Hwang, D.K., Hsu, C.H., Lin, T.C., Chiou, S.H., Chen, S.J., 2016. Laminin modification subretinal bio-scaffold remodels retinal pigment epithelium-driven microenvironment in vitro and in vivo. *Oncotarget* 7, 64631–64648 PubMed ID 27564261.
- Plantner, J.J., Hara, S., Kean, E.L., 1982. Improved, rapid radioimmunoassay for rhodopsin. *Exp. Eye Res.* 35, 543–548 PubMed ID 7151888.
- Radtke, N.D., Aramant, R.B., Petry, H.M., Green, P.T., Pidwell, D.J., Seiler, M.J., 2008. Vision improvement in retinal degeneration patients by implantation of retina together with retinal pigment epithelium. *Am. J. Ophthalmol.* 146, 172–182 PubMed ID 18547537.
- Radtke, N.D., Seiler, M.J., Aramant, R.B., Petry, H.M., Pidwell, D.J., 2002. Transplantation of intact sheets of fetal neural retina with its retinal pigment epithelium in retinitis pigmentosa patients. *Am. J. Ophthalmol.* 133, 544–550 PubMed ID 11931789.
- Saari, J.C., Bunt-Milam, A.H., Bredberg, D.L., Garwin, G.G., 1984. Properties and immunocytochemical localization of three retinoid-binding proteins from bovine retina. *Vis. Res.* 24, 1595–1603 PubMed ID 6398562.
- Sagduullaev, B.T., Aramant, R.B., Seiler, M.J., Woch, G., McCall, M.A., 2003. Retinal transplantation-induced recovery of retinotectal visual function in a rodent model of retinitis pigmentosa. *Invest. Ophthalmol. Vis. Sci.* 44, 1686–1695 PubMed ID 12657610.
- Sanges, D., Simonte, G., Di Vicino, U., Romo, N., Pinilla, I., Nicolas, M., Cosma, M.P., 2016. Reprogramming Muller glia via in vivo cell fusion regenerates murine photoreceptors. *J. Clin. Invest.* 126, 3104–3116 PubMed ID 27427986.
- Santos-Ferreira, T., Llonch, S., Borsch, O., Postel, K., Haas, J., Ader, M., 2016. Retinal transplantation of photoreceptors results in donor-host cytoplasmic exchange. *Nat. Commun.* 7, 13028 PubMed ID 27701381.
- Schwartz, S.D., Regillo, C.D., Lam, B.L., Elliott, D., Rosenfeld, P.J., Gregori, N.Z., Hubschman, J.P., Davis, J.L., Heilwell, G., Sporn, M., Maguire, J., Gay, R., Bateman, J., Ostrick, R.M., Morris, D., Vincent, M., Anglade, E., Del Priore, L.V., Lanza, R., 2015. Human embryonic stem cell-derived retinal pigment epithelium in patients with age-related macular degeneration and Stargardt's macular dystrophy: follow-up of two open-label phase 1/2 studies. *Lancet* 385, 509–516 PubMed ID 25458728.
- Schwartz, S.D., Tan, G., Hosseini, H., Nagiel, A., 2016. Subretinal transplantation of embryonic stem cell-derived retinal pigment epithelium for the treatment of macular degeneration: an assessment at 4 years. *Invest. Ophthalmol. Vis. Sci.* 57 ORSFC1-9. PubMed ID 27116660.
- Seiler, M.J., Aramant, R.B., 1994. Photoreceptor and glial markers in human embryonic retina and in human embryonic retinal transplants to rat retina. *Brain Res Dev Brain Res* 80, 81–95 PubMed ID 7955364.
- Seiler, M.J., Aramant, R.B., 1998. Intact sheets of fetal retina transplanted to restore damaged rat retinas. *Invest. Ophthalmol. Vis. Sci.* 39, 2121–2131 PubMed ID 9761291.
- Seiler, M.J., Aramant, R.B., 2012. Cell replacement and visual restoration by retinal sheet transplants. *Prog. Retin. Eye Res.* 31, 661–687 PubMed ID PMC3472113.
- Seiler, M.J., Aramant, R.B., Jones, M.K., Ferguson, D.L., Bryda, E.C., Keirstead, H.S., 2014. A new immunodeficient pigmented retinal degenerate rat strain to study transplantation of human cells without immunosuppression. *Graefes Arch. Clin. Exp. Ophthalmol.* 252, 1079–1092 PubMed ID 24817311.
- Seiler, M.J., Aramant, R.B., Thomas, B.B., Peng, Q., Sada, S.R., Keirstead, H.S., 2010. Visual restoration and transplant connectivity in degenerate rats implanted with retinal progenitor sheets. *Eur. J. Neurosci.* 31, 508–520 PubMed ID 20105230.
- Seiler, M.J., Lin, R.E., McLelland, B.T., Mathur, A., Lin, B., Sigman, J., De Guzman, A.T., Kitzes, L.M., Aramant, R.B., Thomas, B.B., 2017. Vision recovery and connectivity by fetal retinal sheet transplantation in an immunodeficient retinal degenerate rat model - sheet transplants recover vision in RD nude rats. *Invest. Ophthalmol. Vis. Sci.* 58, 614–630 PubMed ID 28129425.
- Shirai, H., Mandai, M., Matsushita, K., Kuwahara, A., Yonemura, S., Nakano, T., Assawachananont, J., Kimura, T., Saito, K., Terasaki, H., Eiraku, M., Sasai, Y., Takahashi, M., 2016. Transplantation of human embryonic stem cell-derived retinal tissue in two primate models of retinal degeneration. *Proc. Natl. Acad. Sci. U. S. A.* 113, E81–E90 PubMed ID 26699487.

- Silverman, M.S., Hughes, S.E., Valentino, T.L., Liu, Y., 1992. Photoreceptor transplantation: anatomic, electrophysiologic, and behavioral evidence for the functional reconstruction of retinas lacking photoreceptors. *Exp. Neurol.* 115, 87–94 PubMed ID 1728579.
- Singh, M.S., Balmer, J., Barnard, A.R., Aslam, S.A., Moralli, D., Green, C.M., Barnea-Cramer, A., Duncan, I., MacLaren, R.E., 2016. Transplanted photoreceptor precursors transfer proteins to host photoreceptors by a mechanism of cytoplasmic fusion. *Nat. Commun.* 7, 13537 PubMed ID PMC5141374.
- Thliveris, J.A., Yatscoff, R.W., Lukowski, M.P., Copeland, K.R., 1991. Cyclosporine nephrotoxicity—experimental models. *Clin. Biochem.* 24, 93–95 PubMed ID 2060140.
- Thomas, B.B., Seiler, M.J., Sadda, S.R., Aramant, R.B., 2004. Superior colliculus responses to light - preserved by transplantation in a slow degeneration rat model. *Exp. Eye Res.* 79, 29–39 PubMed ID 15183098.
- Walia, S., Fishman, G.A., 2009. Natural history of phenotypic changes in Stargardt macular dystrophy. *Ophthalmic Genet.* 30, 63–68 PubMed ID 19373676.
- West, E.L., Pearson, R.A., Barker, S.E., Luhmann, U.F., MacLaren, R.E., Barber, A.C., Duran, Y., Smith, A.J., Sowden, J.C., Ali, R.R., 2010. Long-term survival of photoreceptors transplanted into the adult murine neural retina requires immune modulation. *Stem cells (Dayton, Ohio)* 28, 1997–2007 PubMed ID 20857496.
- West, E.L., Pearson, R.A., Tschernutter, M., Sowden, J.C., MacLaren, R.E., Ali, R.R., 2008. Pharmacological disruption of the outer limiting membrane leads to increased retinal integration of transplanted photoreceptor precursors. *Exp. Eye Res.* 86, 601–611 PubMed ID 18294631.
- Woch, G., Aramant, R.B., Seiler, M.J., Sagdullaev, B.T., McCall, M.A., 2001. Retinal transplants restore visually evoked responses in rats with photoreceptor degeneration. *Invest. Ophthalmol. Vis. Sci.* 42, 1669–1676 PubMed ID 11381076.
- Yang, P.B., Seiler, M.J., Aramant, R.B., Yan, F., Mahoney, M.J., Kitzes, L.M., Keirstead, H.S., 2010. Trophic factors GDNF and BDNF improve function of retinal sheet transplants. *Exp. Eye Res.* 91, 727–738 PubMed ID 20804751.
- Zhong, X., Gutierrez, C., Xue, T., Hampton, C., Vergara, M.N., Cao, L.H., Peters, A., Park, T.S., Zambidis, E.T., Meyer, J.S., Gamm, D.M., Yau, K.W., Canto-Soler, M.V., 2014. Generation of three-dimensional retinal tissue with functional photoreceptors from human iPSCs. *Nat. Commun.* 5, 4047 PubMed ID 24915161.